An Insight into the Molecular Basis of Salt Tolerance of L-*myo*-Inositol 1-P Synthase (PcINO1) from *Porteresia coarctata* (Roxb.) Tateoka, a Halophytic Wild Rice[1]

Krishnarup Ghosh Dastidar, Susmita Maitra, Lily Goswami, Debjani Roy, Kali Pada Das, and Arun Lahiri Majumder*

Plant Molecular and Cellular Genetics (K.G.D., S.M., L.G., A.L.M.), Bioinformatics Center (D.R.), and Department of Chemistry (K.P.D.), Bose Institute, Calcutta Improvement Trust Scheme-VIIM, Calcutta 700 054, India

The molecular basis of salt tolerance of L-*myo*-inositol 1-P synthase (MIPS; EC 5.5.1.4) from *Porteresia coarctata* (Roxb.) Tateoka (*PcINO1*, AF412340) earlier reported from this laboratory, has been analyzed by in vitro mutant and hybrid generation and subsequent biochemical and biophysical studies of the recombinant proteins. A 37-amino acid stretch between Trp-174 and Ser-210 has been confirmed as the salt-tolerance determinant domain in PcINO1 both by loss or gain of salt tolerance by either deletion or by addition to salt-sensitive MIPS(s) of Oryza (OsINO1) and *Brassica juncea* (BjINO1). This was further verified by growth analysis under salt environment of *Schizosaccharomyces pombe* transformed with the various gene constructs and studies on the differential behavior of mutant and wild proteins by Trp fluorescence, aggregation, and circular dichroism spectra in the presence of salt. 4,4′-Dianilino-1,1′-binaphthyl-5,5-disulfonic acid binding experiments revealed a lower hydrophobic surface on PcINO1 than OsINO1, contributed by this 37-amino acid stretch explaining the differential behavior of OsINO1 and PcINO1 both with respect to their enzymatic functions and thermodynamic stability in high salt environment. Detailed amino acid sequence comparison and modeling studies revealed the interposition of polar and charged residues and a well-connected hydrogen-bonding network formed by Ser and Thr in this stretch of PcINO1. On the contrary, hydrophobic residues clustered in two continuous stretches in the corresponding region of OsINO1 form a strong hydrophobic patch on the surface. It is conceivable that salt-tolerant MIPS proteins may be designed out of the salt-sensitive plant MIPS proteins by replacement of the corresponding amino acid stretch by the designated 37-amino acid stretch of PcINO1.

Metabolic engineering is an effective technology for developing genetically modified stress-tolerant organisms through the production of stress-tolerant determinants like osmolytes/osmoprotectants. Specifically, engineering the structural genes coding for enzymes responsible for biosynthesis of compatible solutes or osmolytes to develop abiotic stress-tolerant transgenic plants has become widespread in the field of stress biology (Hasegawa et al., 2000). Apart from a number of various compounds such as Pro, Gly betaine, trehalose, and sugar alcohols like mannitol, etc. (Hasegawa et al., 2000), the ubiquitous inositol, a six-membered cyclohexitol, and its other derivatives have been implicated to play a vital role in osmotolerance (Bohnert et al., 1995) in addition to its known function in other physiological processes such as cell signaling, membrane biogenesis, growth regulation, phosphorous storage, and as a high-energy phosphate donor (Biswas et al., 1984; Loewus and Murthy, 2000).

Of the eight possible geometrical isomers, *myo*-inositol is the most abundant in the biological system and occupies the central position in inositol metabolism (Bohnert et al., 1995; Loewus and Murthy, 2000; Majumder et al., 2003). De novo biosynthesis of free *myo*-inositol follows a highly conserved two-step biochemical pathway in all living organisms and is catalyzed by L-*myo*-inositol 1-P synthase (MIPS; EC 5.5.1.4). The MIPS converts D-Glc 6-P to L-*myo*-inositol 1-P, and is followed by its dephosphorylation by a specific Mg^{2+}-dependent inositol monophosphatase leading to free inositol (Majumder et al., 2003). This free inositol can then be channeled to the production of different methylated derivatives, which are also active as potent osmolytes for amelioration of oxidative damage during osmotic stress (Bohnert et al., 1995). In addition, *myo*-inositol is known to be utilized in the abiotic stress-induced galactinol and raffinose synthesis (Taji et al., 2002) apart from several other metabolic sinks of its utilization such as the alternate biosynthetic pathway to L-ascorbic acid (Lorence et al., 2004) or the pentosyl or uronosyl component of the plant cell

wall (Kanter et al., 2005). The MIPS has been reported from more than 70 different organisms so far including a wide variety of prokaryotic, archaeal, cyanobacterial, and eukaryotic sources. The structural gene for MIPS, termed *INO1*, has been cloned from a number of widely different organisms that seem to share an evolutionary conserved core catalytic domain across phyla (Majumder et al., 2003).

An increase in the production of intracellular inositol and its other methylated derivatives, such as ononitol and pinitol, as a result of the coordinate transcriptional induction of the *INO1* and the inositol methyl transferase (*Imt1*) gene(s) for increased salt tolerance have been reported in several plants including transgenic ones (Vernon and Bohnert, 1992; Ishitani et al., 1996; Sheveleva et al., 1997; Nelson et al., 1998). Alternatively, increased production of inositol can be achieved even under salt environment by a stress-tolerant MIPS protein by virtue of its ability to remain functional under such condition. This has been documented earlier from this laboratory through isolation and characterization of a novel salt-tolerant MIPS coding gene, termed *PcINO1* from the halophytic wild rice, *Porteresia coarctata* (Roxb.) Tateoka (Majee et al., 2004). In vitro and in vivo characterization revealed that the *PcINO1* gene product is capable of retaining its enzymatic function even in presence of 500 mm NaCl as opposed to its salt-sensitive homolog from the cultivated rice (*Oryza sativa*; *OsINO1*; AB012107). Functional expression of this gene in planta led to a salt-tolerant phenotype of the transgenic tobacco (*Nicotiana tabacum*) with an increased intracellular inositol pool under salt stress, suggesting retention of enzymatic activity of the expressed gene product in vivo. Although a 37-amino acid residue stretch in PcINO1 was found to be primarily responsible for its salt-tolerant characteristics (Majee et al., 2004), an insight into the molecular basis of salt tolerance of this unique enzyme protein as determined by the 37-amino acid residue stretch, was still awaited.

In this study, we have established the importance of the 37-amino acid stretch of PcINO1 offering an insight into the molecular basis of the salt-tolerant characteristics of this protein through biochemical and biophysical characterization of different in vitro generated mutant and hybrid enzymes. This was followed by comparison of the properties of these mutant proteins with those of the wild as well as the salt-sensitive rice homolog, OsINO1, and modeling studies with yeast (*Saccharomyces cerevisiae*) MIPS crystal structure as a template. Furthermore, we have also been able to design a salt-tolerant MIPS out of a salt-sensitive one with this 37-amino acid stretch pointing toward a possible biotechnological application of such studies in the future.

For the sake of uniformity, a new gene nomenclature of *INO1* has been adopted in this manuscript, e.g. *OsINO1* for the cultivated rice *INO1* and *PcINO1* for *Porteresia coarctata INO1*, in place of earlier *RINO1* or *PINO1* nomenclature (Majee et al., 2004). The chimeric proteins have been designated as Os::PcINO1 or Bj::PcINO1, wherein a part of PcINO1 has been inserted onto OsINO1 or BjINO1.

RESULTS

Generation and Molecular Cloning of ΔPcINO1.1, ΔPcINO1.2, Os::PcINO1, BjINO1, and Bj::PcINO1

Strategy of generating *ΔPcINO1.1*, *ΔPcINO1.2*, *Os::PcINO1*, and *Bj::PcINO1* has been schematically described in Figure 1. In the case of *ΔPcINO1.1* (Fig. 1B), a stretch of 60 nucleotides coding for 20 amino acids from Asn-342 to Lys-361 near the C terminus of PcINO1 has been deleted. This stretch is part of the identified core catalytic domain of MIPS (Majumder et al., 2003) and harbors two important Lys residues implicated in the catalytic mechanism of MIPS reaction (Stein and Geiger, 2002). For generating *ΔPcINO1.2* (Fig. 1B), a 111-bp stretch corresponding to a 37-amino acid residue stretch between Trp-174 and Ser-210 has been deleted from near the N terminus of PcINO1 without affecting the MIPS catalytic activity. In the case of *Os::PcINO1* (Fig. 1C), the advantage of having two unique restriction sites, *Pst*I and *Eco*RV in both the *OsINO1* and *PcINO1* genes at the same position has been exploited. The *Pst*I-*Eco*RV fragment corresponds to a peptide larger than 37-amino acid residue stretch that includes additionally the flanking sequences at both sides of the Trp-174 to Ser-210 stretch that are identical in both the OsINO1 and PcINO1 proteins. Therefore, replacing the *Pst*I-*Eco*RV fragment of *OsINO1* with that of *PcINO1* essentially replaced the 37-amino acid stretch of OsINO1 with that of PcINO1. The corresponding 37-amino acid stretch of BjINO1, which showed approximately 98% and 55% sequence identity with *Brassica napus* (AAB06756) and *S. cerevisiae* (A30902) MIPS, respectively, has been replaced with the same of PcINO1 by PCR to generate Bj::PcINO1 (Fig. 1D).

Functional Complementation of ΔPcINO1.1, ΔPcINO1.2, and Os::PcINO1

Functional viability of each *PcINO1* mutant and hybrid genes have been tested by the yeast functional complementation assay as described earlier (Chatterjee et al., 2004; Majee et al., 2004). Results of such experiments (Fig. 2) reveal that, except for the *ΔPcINO1.1*, all mutants and hybrid genes complemented the *FY250* strain, thereby adducing evidence that the changes made in the constructs by in vitro mutagenesis did not alter the MIPS catalytic activity in any of them. We subcloned *ΔPcINO1.1*, *ΔPcINO1.2*, and *Os::PcINO1* downstream of a strong constitutively active glyceraldehyde 3-P dehydrogenase (GPD) promoter in yeast multicopy binary vector p426GPD (Sambrook et al., 1989; Mumberg et al., 1995), followed by transformation of *FY250* with *p426GPD* (negative control) along with the respective constructs. All the transformants were
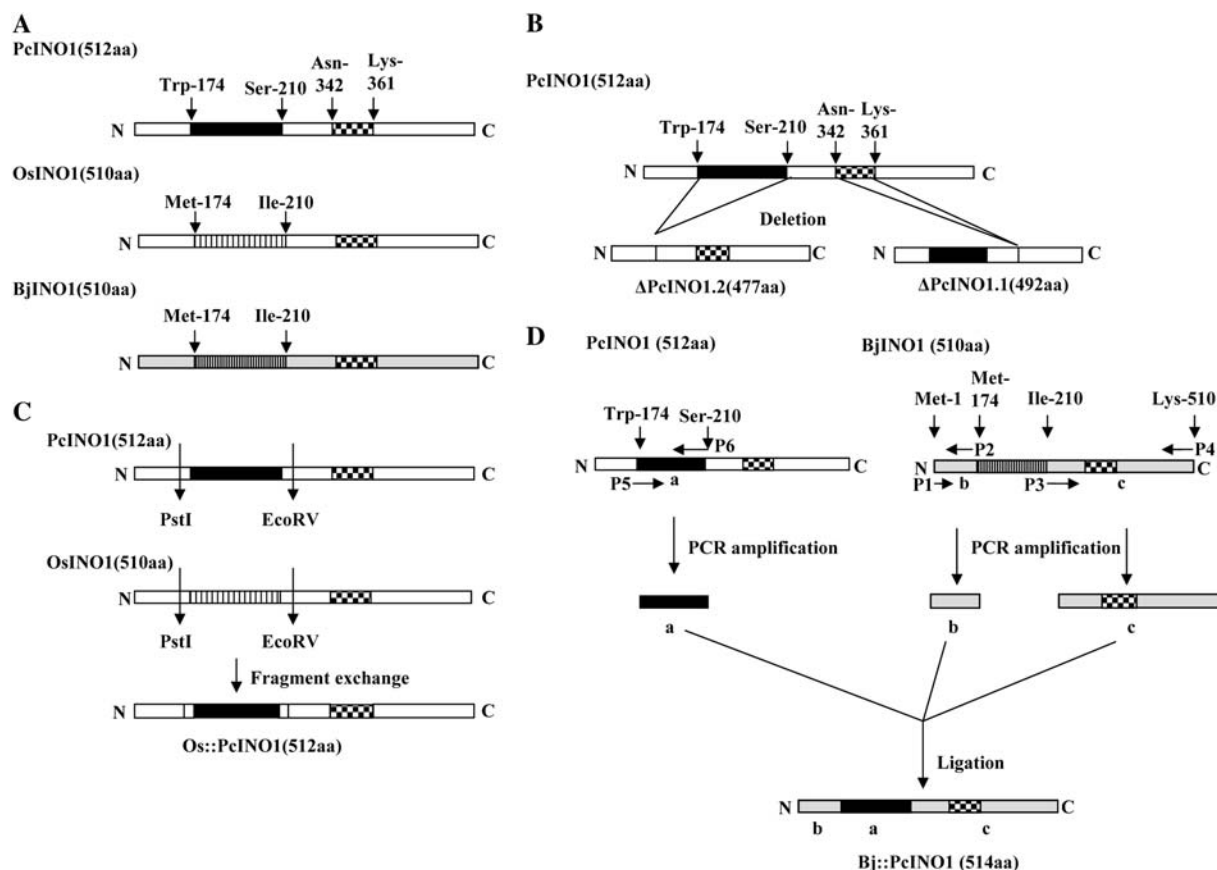
Figure 1. Scheme for development of different *PcINO1* mutants, *BjINO1*, *Os*::*PcINO1*, and *Bj*::*PcINO1*. A, Schematic representation of *PcINO1*, *OsINO1*, and *BjINO1*. B, Strategy of generating deletion mutants Δ*PcINO1.2* and Δ*PcINO1.1* by PCR. C, *Os*::*PcINO1* by fragment exchange method. D, *Bj*::*PcINO1* by PCR. The major difference between OsINO1 or BjINO1 with PcINO1, as highlighted by different shading, is the 37-amino acid residue stretch (Trp-174 to Ser-210). A part of the core catalytic region (20-amino acid residue stretch) is also highlighted (Asn-342 to Lys-361). Deletion of the 37-amino acid residue stretch resulted in ΔPcINO1.2 and deletion of the 20-amino acid residue stretch resulted in ΔPcINO1.1. Replacing the corresponding 37-amino acid residue stretch from OsINO1 with that of PcINO1 generated the hybrid Os::PcINO1 or Bj::PcINO1.

selected on uracil dropout medium and maintained on solid synthetic media containing no uracil and 10 μM inositol where all grew equally well (Fig. 2A). However, when inositol concentration was gradually lowered down to zero, only *PcINO1* (Fig. 2B, 5), Δ*PcINO1.2* (Fig. 2B, 4), and *Os*::*PcINO1* (Fig. 2B, 3) transformed cells showed growth whereas *p426GPD* (Fig. 2B, 1) and Δ*PcINO1.1*(Fig. 2B, 2) transformed cells showed no growth.

Elucidating Salt-Tolerant Phenotype of *PcINO1*-Transformed *Schizosaccharomyces pombe*

Functional expression of *PcINO1* has earlier been reported to confer salt-tolerant phenotype with unabated photosynthetic functions to transformed tobacco plants, a model photosynthetic system (Majee et al., 2004). Following such observations, we attempted functional expression of *PcINO1*, *OsINO1*, Δ*PcINO1.2*, and *Os*::*PcINO1* hybrid genes under salt-stressed conditions to see their effect on the growth of a non-

photosynthetic lower eukaryote, *S. pombe*. Being a natural inositol auxotroph, which requires approximately 50 to 55 μM basal level of inositol for its normal growth (Ingavale and Bachhawat, 1999), *S. pombe* presents a model system for in vivo complementation as well as for studying the effect of functional expression of the genes *PcINO1*, *OsINO1*, Δ*PcINO1.2*, and *Os*::*PcINO1* on the growth of the organism in salt environment. However in this experiment, since the cells were given salt stress, a basal level of 2 μM inositol has been maintained throughout along with the increasing concentration of NaCl. In absence of any salt or at lower salt concentrations like 100 mM, transformed cells showed more or less similar growth pattern (Fig. 3, A and B). But on increasing NaCl stress beyond 100 mM NaCl, a remarkable difference in growth pattern of the transformed cells was observed. *S. pombe* cells transformed with *OsINO1* and Δ*PcINO1.2* showed poor growth response when grown with further increase in NaCl concentration as opposed to *PcINO1*- and *Os*::*PcINO1*-transformed cells, which were found to grow even in presence of 500 mM NaCl (Fig. 3, C–F).
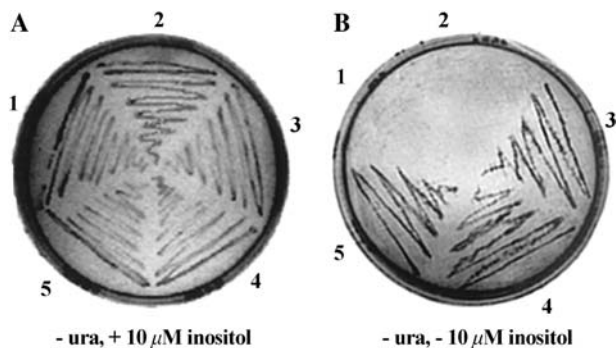
Figure 2. Functional complementation of mutant genes of *PcINO1* and the hybrid derivative of *OsINO1* in *S. cerevisiae FY250*, an inositol auxotroph. A, Growth of *FY250*-transformed cells with empty vector, *p426GPD* (1, −control), *ΔPcINO1.1* (2), *Os::PcINO1* (3), *ΔPcINO1.2* (4), and *PcINO1* (5, +control) on complete synthetic solid media in presence of 10 μM inositol in absence of uracil (ura). B, Growth of transformed cells as in A above in absence of both inositol and uracil (ura).

Although extent of growth was found to be reduced even in the case of *PcINO1*- and *Os::PcINO1*-transformed cells at 500 mM NaCl concentration, in the case of *OsINO1* and *ΔPcINO1.2* transformants, virtually no growth was observed at similar salt concentration.

Bacterial Overexpression, Purification, and in Vitro MIPS Activity of Recombinant ΔPINO1.1, ΔPINO 1.2, Os::PcINO1, BjINO1, and Bj::PcINO1 Proteins

ΔPcINO1.1, *ΔPcINO1.2*, *BjINO1*, *Os::PcINO1*, and *Bj::PcINO1* were overexpressed as approximately 60-kD proteins, predominantly in the particulate fraction, as judged by the 10% SDS-PAGE and western-blot analysis of respective supernatant and pellet of induced cells (Fig. 4, A–D). In both SDS-PAGE and western-blot analysis, a slight decrease in the M_r of overexpressed

protein bands were observed commensurate with the size of ΔPcINO1.1 and ΔPcINO1.2 with the deletion of 20- and 37-amino acid residue stretches, respectively.

The overexpressed ΔPcINO1.1, ΔPcINO1.2, Os::PcINO1, BjINO1, and Bj::PcINO1 proteins were purified to homogeneity and assayed for MIPS activity following the procedure described earlier (Majee et al., 2004). When in vitro specific activity was determined using approximately 20 μg of each purified enzyme, both ΔPcINO1.2 and Os::PcINO1 were found to be almost as active as wild PcINO1 and OsINO1 (positive controls), as opposed to ΔPcINO1.1, which turned out to be inactive (Fig. 4E). Bj::PcINO1 was also found to be equally active as BjINO1 (Fig. 4E) and very close to those of OsINO1 and PcINO1. Both purified ΔPcINO1.2 and Os::PcINO1 proteins were biochemically characterized and compared with their corresponding wild versions (Table I). K_m and V_{max} for D-Glc 6-P and NAD$^+$ of purified ΔPcINO1.2 and Os::PcINO1 were found to be comparable to those of the wild OsINO1 and PcINO1 proteins. Os::PcINO1 was found to be optimally active slightly in the higher pH range (8.0–8.5) in comparison to wild proteins.

In Vitro Salt Tolerance versus Sensitivity of Mutant and Hybrid Proteins

We earlier showed that with increasing concentration of NaCl, the MIPS activity of PcINO1 remained unaltered but that of OsINO1 progressively decreased (Majee et al., 2004). The 37-amino acid residue stretch deficient mutant of PcINO1 (ΔPcINO1.2) or BjINO1 was found to behave as OsINO1, showing a steady decrease in MIPS activity with increased salt concentration (Fig. 4F). On the other hand, the hybrid Os::PcINO1 and Bj::PcINO1, in which the 37-amino acid residue stretch of PcINO1 replaces the

Figure 3. Phenotypic expression of different PcI-NO1 genes in *S. pombe*. A to F, Growth pattern of *S. pombe PR109*, transformed with different pREP1 constructs harboring *OsINO1*, *PcINO1*, *ΔPcINO1.2*, and *Os::PcINO1* genes on complete solid synthetic media containing increasing concentration of NaCl, as indicated. 1, Empty vector, *pREP1*; 2, *OsINO1*; 3, *Os::PcINO1*; 4, *ΔPcINO1.2*; and 5, *PcINO1*.
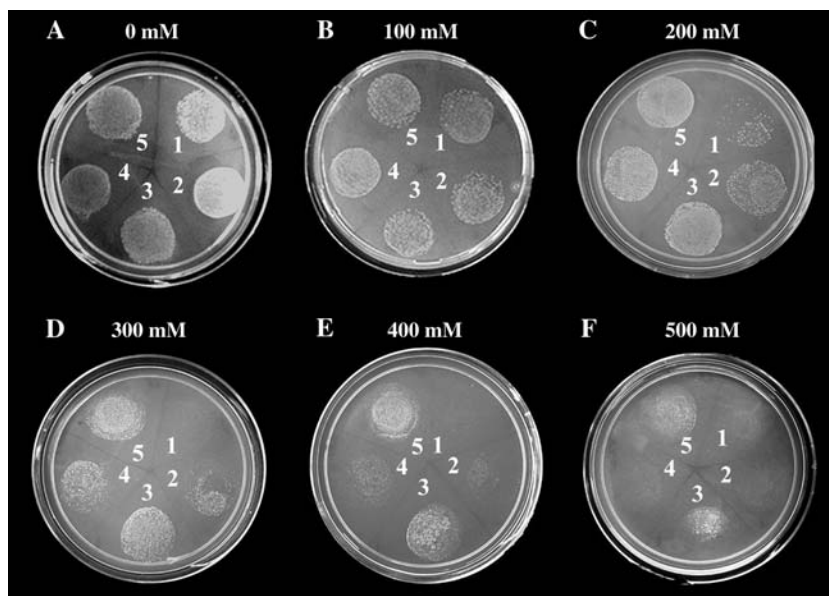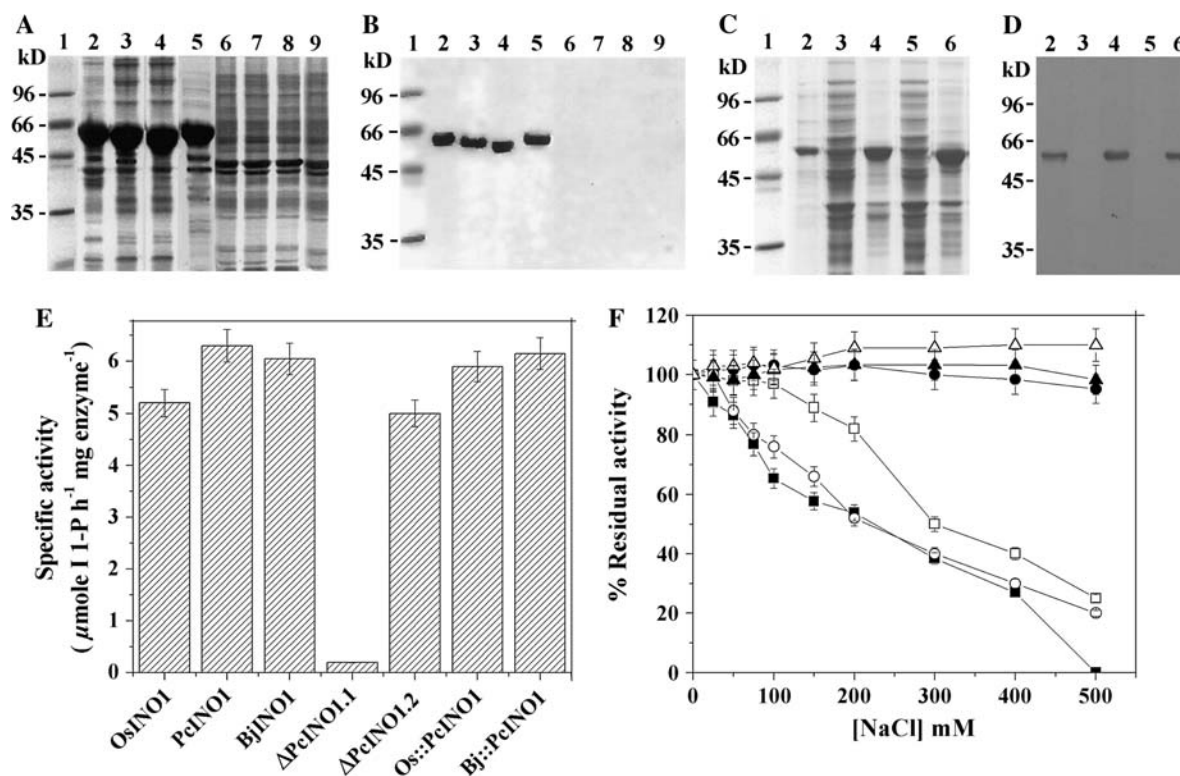
Figure 4. Bacterial expression and western-blot analysis of various PcINO1 mutants, Os::PcINO1, BjINO1, and Bj::PcINO1 gene products, their in vitro MIPS activity, and salt tolerance vis à vis salt sensitivity. A and C, Ten-percent SDS-PAGE. B and D, Corresponding western-blot analysis of PcINO1 mutants, Os::PcINO1, BjINO1, and Bj::PcINO1, respectively. A and B, Lane 1, M_r marker; lanes 2 to 5, pellet fractions of overexpressed PcINO1, ΔPcINO1.1, ΔPcINO1.2, and Os::PcINO1, respectively; lanes 6 to 9, corresponding supernatants, respectively. C and D, Lane 1, M_r marker; lane 2, OsINO1 (+ control); lanes 3 and 4, induced BjINO1 supernatant and pellet fractions, respectively; lanes 5 and 6, induced Bj::PcINO1 supernatant and pellet fractions, respectively. E, In vitro MIPS activity of purified PcINO1 mutants, Os::PcINO1, BjINO1, and Bj::PcINO1 along with the positive controls PcINO1 and OsINO1. Specific activity is described in terms of μmol inositol 1-P h^{-1} mg protein^{-1}. In each case 20 μg purified protein was taken. Error bars indicate the deviation of triplicate experiments. F, Effect of increasing concentration of NaCl on the MIPS activity of ΔPcINO1.2 (white circle), Os::PcINO1 (black triangle), BjINO1 (white square), Bj::PcINO1 (white triangle), along with OsINO1 (−control, black square) and PcINO1 (+control, black circle). Approximately 20 μg of each purified enzyme was assayed in presence of indicated concentration of NaCl. Error bars indicate the deviation from triplicate experiments.

corresponding 37-amino acid residue stretch of OsINO1 or BjINO1, behave like PcINO1 showing no decrease in MIPS catalytic activity on increasing salt concentration up to 500 mM (Fig. 4F). These results clearly indicate that the specific 37-amino acid residue stretch from Trp-174 to Ser-210 of PcINO1 provides the salt-tolerance property to Os::PcINO1 and Bj::PcINO1 and its absence is responsible for the salt sensitivity of ΔPcINO1.2, OsINO1, and BjINO1.

Trp Fluorescence Studies of Mutant and Hybrid Proteins in the Presence and Absence of NaCl

We showed earlier that with increasing salt concentration, Trp fluorescence intensity of OsINO1 decreased significantly but that of PcINO1 decreased negligibly (Majee et al., 2004). The Trp emission spectra of the mutant and hybrid proteins in presence of increasing concentration of NaCl have been shown in

Table I. *Comparison of biochemical properties of ΔPcINO1.2 and Os::PcINO1 with their wild enzymes*

System	K_m		V_{max}		pH Optima	Temperature Optima °C
	G-6-P	NAD$^+$	G-6-P	NAD$^+$		
	mM		μmol I 1-P/min			
OsINO1[a]	3.0	0.188	0.072	0.068	7.5	37
PcINO1[a]	2.5	0.166	0.095	0.087	8.0	37
ΔPcINO1.2	2.83	0.451	0.103	0.096	8.0	37
Os::PcINO1	3.19	0.293	0.115	0.081	8.0–8.5	37

[a]Data from Majee et al. (2004).

Figure 5, A and B. We found that the fluorescence intensity of the mutant protein ΔPcINO1.2 protein became highly sensitive to the concentration of NaCl, like OsINO1, the intensity being quenched without change of emission maximum as NaCl concentration was increased. The lower Trp intensity observed for ΔPcINO1.2 (Fig. 5A) compared to PcINO1 in absence of added NaCl might be due to the presence of two additional Trp residues in the 37-amino acid residue stretch of PcINO1, in comparison to ΔPcINO1.2. The Os::PcINO1, like PcINO1, did not show any appreciable quenching of Trp fluorescence in presence of NaCl (Fig. 5B).

An anion such as iodide ion acts as a collisional quencher, but its quenching ability depends upon the ionic charge distribution near the Trp residues (Eftink and Ghiron, 1981; Lakowicz, 1983). Chloride ion is of smaller size than iodide with a higher penetration capability than iodide, and therefore can quench those Trps located close to the surface. The lack of shift of emission maximum revealed that NaCl was unable to alter the polarity of the Trp microenvironment since the fluorescence-contributing Trp are not fully exposed to aqueous environment. Therefore, the salt-induced quenching of Trp fluorescence of OsINO1 and ΔPcINO1.2 suggests changes in the distribution of neighboring charge groups (Eftink and Ghiron, 1981). We also observed that for OsINO1 and ΔPcINO1.2 the amount of quenching was not strictly proportional to the concentration of quencher, indicating some static quenching as well (Lakowicz, 1983). The static quenching can arise from the binding of NaCl to the proteins (Eftink and Ghiron, 1981; Albany, 2004). This again points toward changes in the ionic environment at the protein surface. Therefore our results suggest that the presence or absence of the 37-amino acid residue stretch of PcINO1 can cause considerable difference in the ionic charge distribution on the protein surface leading to a drastically altered behavior of the proteins in presence and absence of NaCl.

Surface Hydrophobicity of OsINO1, PcINO1, and PcINO1 Mutant and Hybrid Proteins

Surface properties of proteins are extremely important to understand protein-protein interactions and the behavior of proteins under stressed conditions (Fersht, 1999). We have studied the exposure of hydrophobic pockets on the surface of OsINO1 and PcINO1 and their mutants by 4,4′-dianilino-1,1′-binaphthyl-5,5-disulfonic acid (bis-ANS) binding method. Bis-ANS is a conformation-sensitive hydrophobic probe, which is poorly fluorescent in aqueous solution but become highly fluorescent on binding to hydrophobic pockets (Das and Surewicz, 1995; Horowitz et al., 1995; Das et al., 1996). We qualitatively showed earlier that in absence of salt, OsINO1 binds more bis-ANS than PcINO1 (Majee et al., 2004). Here we extended the study through quantitative treatment of surface hydrophobic property to wild and mutant proteins. To quantitatively characterize the number of bis-ANS binding sites and the binding constant, we performed a fluorimetric titration of the proteins by bis-ANS in presence and absence of NaCl. Typical titration results for ΔPcINO1.2 and the Os::PcINO1 proteins both in presence and absence of 500 mM NaCl have been presented in Figure 6A. ΔPcINO1.2 was found to have higher hydrophobicity than the Os::PcINO1 both in presence and absence of NaCl. The data was analyzed by plotting ν versus ν/S according to the Scatchard equation given by:

$$\nu = n - k_d[\nu/S], \qquad (1)$$

assuming n identical noninteracting sites per subunit of these proteins, where ν and S are the concentrations of bound and free bis-ANS (μM), respectively, and n is the number of binding sites and k_d is the dissociation constant.

To convert the change in fluorescence intensity into bound bis-ANS, a reverse titration of bis-ANS by protein solution was performed as described by Cardamone
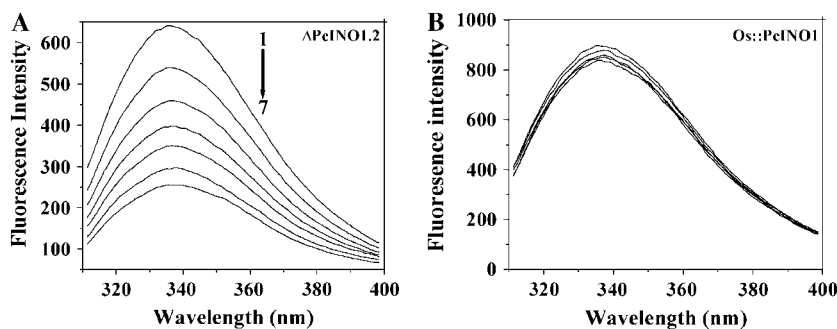
Figure 5. Fluorescence quenching of Trp. Trp fluorescence emission spectra of ΔPcINO1.2 (A) and Os::PcINO1 (B). The excitation wavelength was 295 nm and emission was scanned between 300 to 400 nm. All proteins were in 20 mM Tris-HCl buffer, pH 7.5, containing 10 mM β-ME at a concentration of 0.15 mg/mL and the total reaction mixture was 1 mL. Line 1, Protein alone; line 2, protein + 100 mM NaCl; line 3, protein + 200 mM NaCl; line 4, protein + 300 mM NaCl; line 5, protein + 400 mM NaCl; line 6, protein + 500 mM NaCl; and line 7, protein + 600 mM NaCl. In all cases protein samples either in absence or presence of salt were incubated at 37°C for 10 min before subjected to emission scanning.
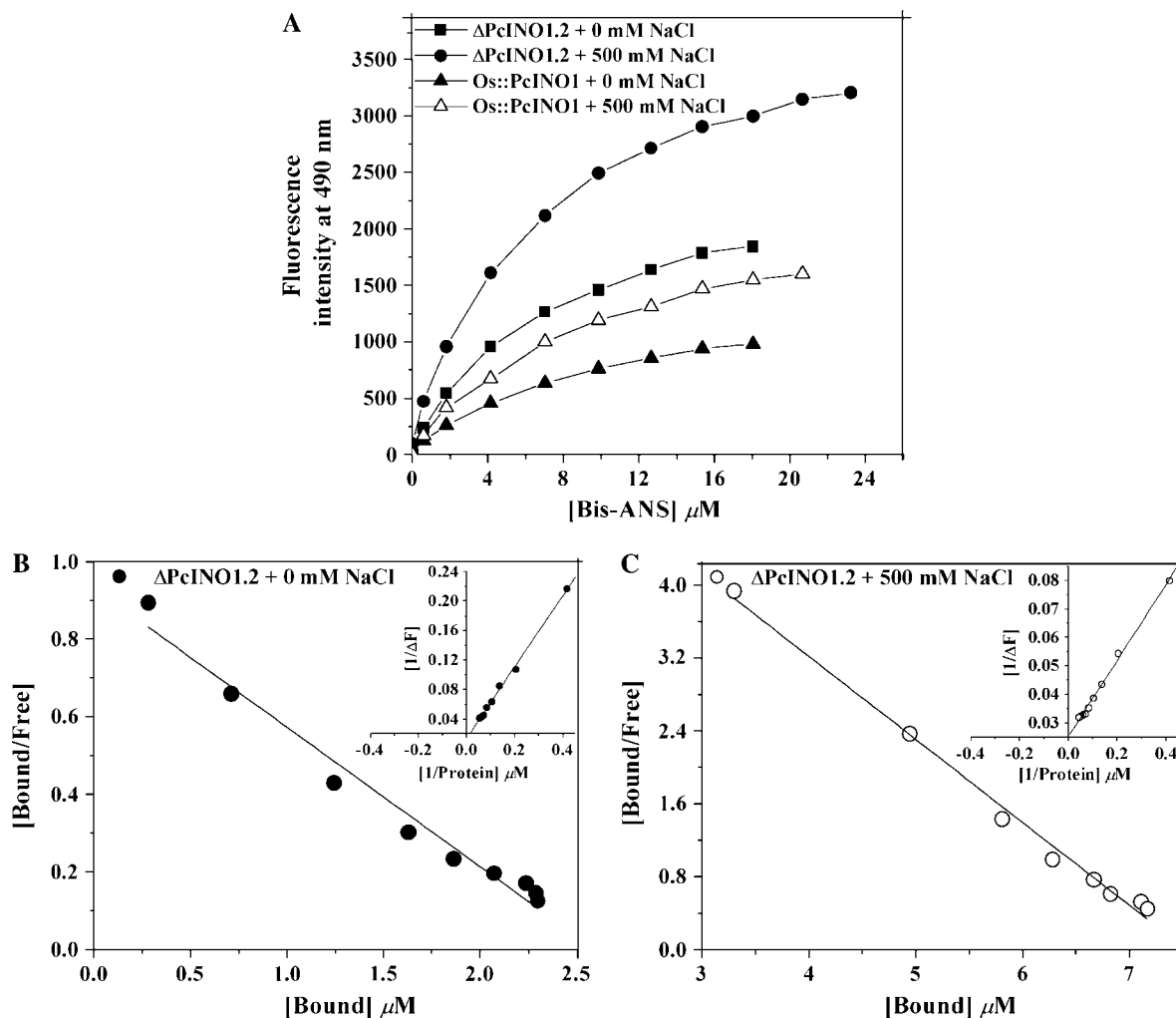
Figure 6. Surface hydrophobicity of PcINO1 mutant proteins. A, Bis-ANS binding titration of ΔPcINO1.2 and Os::PcINO1 in presence and absence of added salt. A total of 0.15 mg/mL of each protein, in 20 mM Tris-HCl (pH 7.5), and 10 mM β-ME was titrated in total 1 mL reaction volume by aqueous solution of bis-ANS. The excitation and emission wavelengths were 390 and 490 nm, respectively. The intensities at 490 nm, from the titration, were plotted as a function of bis-ANS concentration. In both the cases of titration in no salt and salt condition, protein was incubated at 37°C either in absence or presence of salt for 10 min before being subjected to titration. Black square, ΔPcINO1.2 + 0 mM NaCl; black circle, ΔPcINO1.2 + 500 mM NaCl; white triangle, Os::PcINO1 + 0 mM NaCl; and black triangle, Os::PcINO1 + 500 mM NaCl. B and C, Typical representative Scatchard plot of ΔPcINO1.2 for the determination of stoichiometry (n) and the dissociation constant (k_d) in absence (B) and presence (C) of 500 mM NaCl. Respective insets show the double reciprocal plot of reverse titration data as a function of protein concentration for the determination of ΔF_{max}. In reverse titration also, protein samples were incubated at 37°C, either in absence or presence of salt for 10 min before being subjected to titration under no salt and salt conditions, respectively.

and Puri (1992). Typical Scatchard plots for the bis-ANS-ΔPcINO1.2 binding in presence and absence of salt have been shown in Figure 6, B and C. From the slope and intercepts of this plot the number of binding site (n) and dissociation constant for binding (k_d) was calculated. These values for OsINO1, PcINO1, ΔPcINO1.2, and Os::PcINO1 have been presented in Table II. It was observed that both OsINO1 and ΔPcINO1.2 had a huge increase in n when NaCl was increased from 0 to 500 mM. Relatively small changes in n were observed for PcINO1 and Os::PcINO1, decreasing slightly for the former and increasing a little for the latter on moving from no salt to high salt concentra-

tion. The dissociation constant in presence of salt was always found to have increased somewhat than that without salt. From Table II, it is seen that in absence of salt, removal of the 37-amino acid residue stretch of PcINO1 from Trp-174 to Ser-210 led to a marginal decrease of n from 1.25 to 0.94, but in the presence of 500 mM NaCl, n increased approximately 10-fold from 0.7 to 6.9. Therefore the absence of the 37-amino acid residue stretch of PcINO1 in ΔPcINO1.2 shifts the hydrophilic-lipophilic balance of the folded protein to expose hydrophobic sites on its surface in the presence of NaCl. Similarly, when this 37-amino acid residue stretch of PcINO1 replaces that in OsINO1, the number of

Table II. *Determination of stoichiometry (n) and dissociation constant (k_d) of different systems in absence and presence of 500 mM NaCl*

System	n	k_d
		μM
OsINO1 − salt	2.6 ± 0.047	0.684 ± 0.017
OsINO1 + salt	6.32 ± 0.18	1.76 ± 0.063
PcINO1 − salt	1.25 ± 0.0183	0.263 ± 0.0064
PcINO1 + salt	0.7 ± 0.021	0.32 ± 0.014
ΔPcINO1.2 − salt	0.94 ± 0.0412	0.36 ± 0.024
ΔPcINO1.2 + salt	6.9 ± 0.21	0.911 ± 0.034
Os::PcINO1 − salt	0.21 ± 0.004	0.16 ± 0.006
Os::PcINO1 + salt	0.263 ± 0.0063	0.196 ± 0.008

hydrophobic sites decreases in absence of NaCl and more drastically in presence of NaCl. Thus, this 37-amino acid residue stretch is so unique that its presence in PcINO1 and Os::PcINO1 minimizes the structural changes of the proteins in presence of salt but its absence in ΔPcINO1.2 and also in OsINO1 helps change its surface becoming highly hydrophobic.

Aggregation of OsINO1, PcINO1, and PcINO1 Mutant and Hybrid Proteins in the Presence and Absence of NaCl

We showed earlier that in the presence of high salt, OsINO1 forms nonspecific molecular aggregates, while PcINO1 remains unchanged (Majee et al., 2004). To find out the physical basis of salt sensitivity of ΔPcINO1.2 vis à vis salt tolerance of Os::PcINO1, we monitored static light scattering of purified ΔPcINO1.2 (Fig. 7A) and Os::PcINO1 (Fig. 7B) in presence and absence of NaCl both at 37°C and 25°C. At 37°C, along with increase in incubation time, ΔPcINO1.2 showed a steady formation of macromolecular aggregates, which was salt concentration dependent, like OsINO1. In the case of ΔPcINO1.2 both the degree as well as the rate of formation of the aggregates is much faster than those of OsINO1 and increased with the increasing concen-

tration of NaCl. ΔPcINO1.2 reached saturation within 30 min of incubation, whereas OsINO1 reached the same at 140 min. However Os::PcINO1 in all NaCl concentrations showed no aggregation even after 170 min of incubation at 37°C, like PcINO1. At 25°C, the rate as well as extent of aggregation was found to be reduced (data not shown). Aggregation of both OsINO1 and ΔPcINO1.2 was also found to be critically dependant on the protein concentration and reduced to a great extent when protein concentration was below approximately 300 $\mu g/mL$.

Circular Dichroism Spectroscopy in the Presence and Absence of NaCl

To investigate the details of any structural change occurring at the level of secondary structure of these mutants in presence of NaCl we took far-UV circular dichroism (CD) spectra of purified OsINO1, PcINO1, ΔPcINO1.2, and Os::PcINO1 in presence and absence of NaCl at room temperature (Fig. 8, A–D). PcINO1 and the Os::PcINO1 (Fig. 8, A and D) showed distinct α-helical characteristics, which remained fairly unaltered by the addition of salt, while the characteristics of OsINO1 and ΔPcINO1.2 changed with salt (Fig. 8, B and C). In this case the spectrum changed from w shape to v shape but minimum shifted above 220 nm at salt concentration of 500 mM. The spectral data were fitted to several secondary structure analysis programs (Sreerama, 1993; Sreerama et al., 1999) such as SELCON3, CONTIN, CDSSTR, CDNN, etc. The general agreement between the fitted parameters from different programs were not found to be satisfactory, but in most cases an increase in β-sheet structure at the expense of helical structure and increase in random coil contribution was found to be observed (data not shown). The difference in salt effect on the CD characteristics between OsINO1 and Os::PcINO1 as also between PcINO1 and ΔPcINO1.2 indicates that
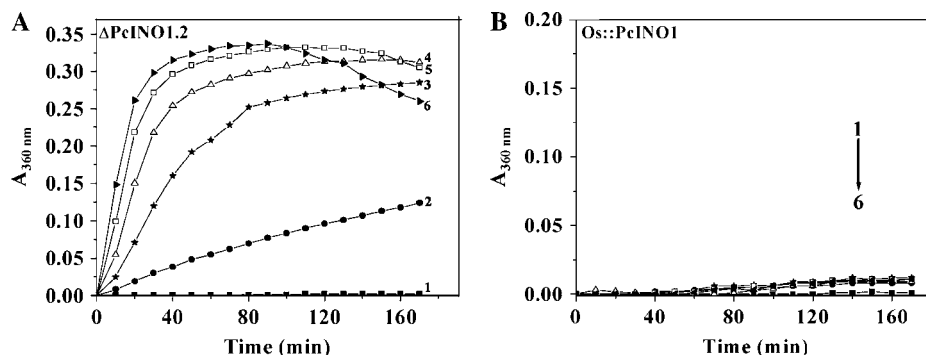
Figure 7. Light scattering property of mutant proteins. Aggregation assay of ΔPcINO1.2 (A) and Os::PcINO1 (B) in different concentration of NaCl. Approximately 300 $\mu g/mL$ of each purified protein in 20 mM Tris-HCl (pH 7.5) and 10 mM β-ME was subjected to static light scattering at 360 nm in absence and presence of increasing concentrations of NaCl (100–500 mM) at 37°C in SHIMADZU UV-160A for up to 170 min. Absorbance values at 360 nm were plotted at 10 min intervals as a function of time. Line 1, 0 mM NaCl; line 2, +100 mM NaCl; line 3, +200 mM NaCl; line 4, +300 mM NaCl; line 5, +400 mM NaCl; and line 6, +500 mM NaCl.
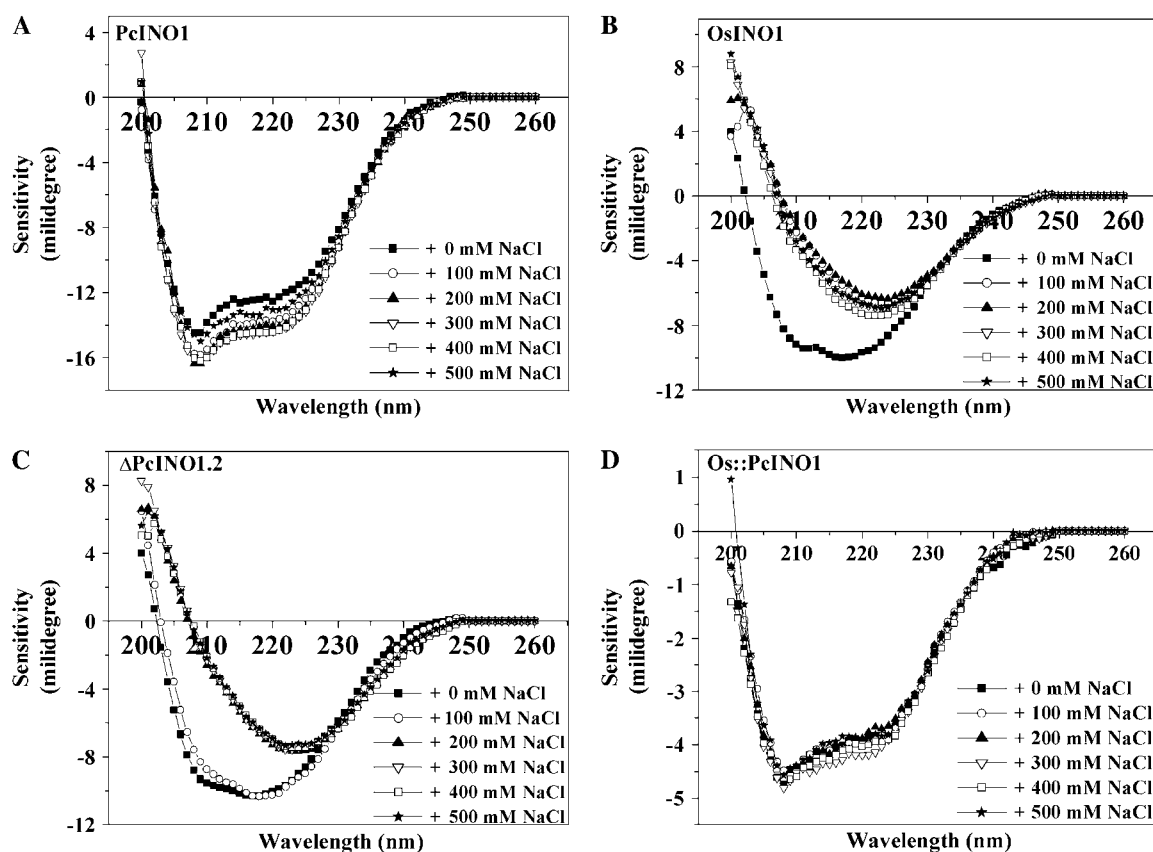
Figure 8. Change in the secondary structure as revealed by CD spectra in OsINO1, PcINO1, and the mutant proteins in the presence of salt. CD profile of PcINO1 (A), OsINO1 (B), ΔPcINO1.2 (C), and Os::PcINO1 (D) in presence and absence of increasing concentration of NaCl at room temperature. All the proteins were in 5 mM sodium phosphate buffer and approximately 0.1 mg/mL protein was used in each experiment. Spectrum was scanned between 260 to 200 nm using 2 mm pathlength cuvette in total 1.5 mL reaction volume. In all experiments, protein samples were incubated for 10 min at 37°C either in absence or presence of increasing concentration of added NaCl.

the CD behavior is dictated by the sequence difference in this 37-amino acid residue stretch.

Thermodynamic Stability of OsINO1/PcINO1 Mutants in the Presence and Absence of NaCl

To understand the thermodynamic basis for the salt tolerance of PcINO1 and Os::PcINO1 and sensitivity of OsINO1 and ΔPcINO1.2, respectively, we analyzed the urea-induced denaturation profiles of these proteins in presence and absence of 500 mM NaCl. The profiles were created by measuring Trp fluorescence of the protein solutions as a function of urea concentration (Biswas and Das, 2004). Since the emission maxima shifted from 337 to over 350 nm as urea concentration increased from 0 to 8 M, the data were plotted as fluorescence intensity ratio (I_{337}/I_{350}) between 337 and 350 nm against urea concentration.

Figure 9, A to D displays the denaturation profiles of PcINO1, OsINO1, ΔPcINO1.2, and Os::PcINO1 in absence and presence of 500 mM NaCl. All these profiles were found to be of sigmoidal shape. From the sigmoidal analysis of the data the urea concentration at which the proteins are 50% denatured ($C_{0.5}$) was obtained. It was found that $C_{0.5}$ for PcINO1 in absence and presence of 500 mM NaCl are 3.2 and 3.3 M urea, respectively, whereas those for OsINO1 in absence and presence of 500 mM NaCl are 3.5 and 4.3 M, respectively. The $C_{0.5}$ of ΔPcINO1.2 and Os::PcINO1 changed from 3.5 to 3.1 M urea in absence of NaCl to 4.0 and 3.8 M urea in presence of 500 mM NaCl. The standard free energy change (ΔG^0) required to fully unfold these proteins from their native state in absence of urea was computed by fitting the experimental denaturation profile according to a three-state model (Das et al., 1995; Sun et al., 1999) as follows:

$$I = \frac{I_0 + I_1 \times \exp(-\Delta G_1^0 + (m_1 \times [\text{urea}])/RT + I_\infty \times \exp(-\Delta G_2^0 + (m_2 \times [\text{urea}])/RT}{1 + \exp(-\Delta G_1^0 + (m_1 \times [\text{urea}])/RT + \exp(-\Delta G_2^0 + (m_2 \times [\text{urea}])/RT}. \tag{2}$$
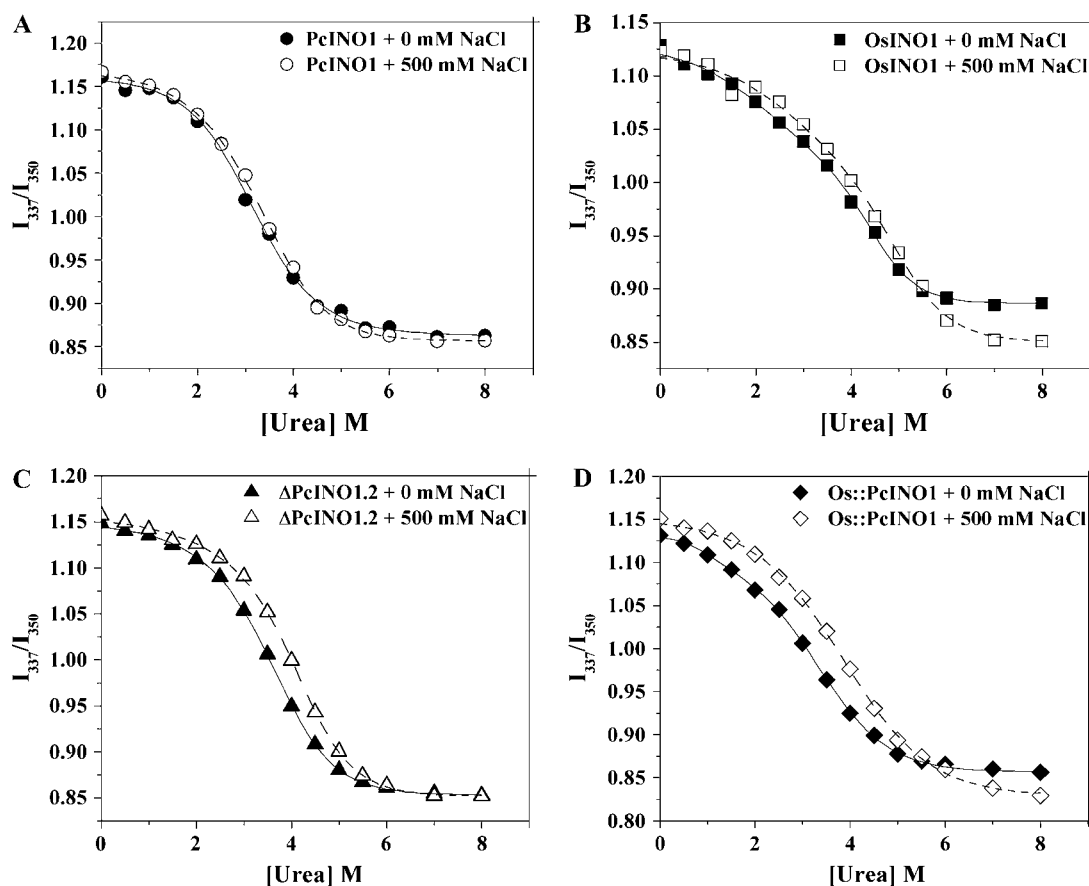
Figure 9. Thermodynamic stability of OsINO1, PcINO1, and the mutant proteins in absence and presence of NaCl. Urea-induced denaturation profile of PcINO1 (A), OsINO1 (B), ΔPcINO1.2 (C), and Os::PcINO1 (D) in absence and presence of 500 mM NaCl at 25°C. All the experiments were done at a protein concentration of 0.05 mg/mL, in 20 mM Tris-HCl (pH 7.5), 10 mM β-ME, and 5% glycerol. In each case protein samples were incubated in increasing concentration of urea (0–8 mM) either in absence or presence of 500 mM NaCl in total 1 mL reaction volume for about 16 h at room temperature 25°C. Samples were excited at 295 nm and emission was scanned between 300 to 400 nm. Ratio of fluorescence intensity at 337 nm to the same at 350 nm was plotted as function of urea concentration.

I_0 is the fluorescence intensity at 0 M urea; I_1 is the fluorescence intensity of the proposed intermediate; I_∞ is the fluorescence intensity at 8 M urea; and ΔG_1^0 and ΔG_2^0 are standard free energy changes of native-to-intermediate and intermediate-to-unfolded state, respectively. m_1 and m_2 are the slopes for the respective processes. ΔG^0 is the sum of ΔG_1^0 and ΔG_2^0, which refers to the standard free energy change between native and unfolded state at zero urea concentration

$(\Delta G_{[\text{Urea}]}^0)$. As per this model, the native state (N) reaches the denatured state (D) via an intermediate state (I) according to $N \leftrightarrow I \leftrightarrow D$. The parameters for this fit have been given in Table III. It was observed from Table III that for all four proteins (OsINO1, PcINO1, ΔPcINO1.2, and Os::PcINO1), ΔG_1^0 are much less than the ΔG_2^0 both in presence and absence of NaCl, indicating that the intermediate is located closer to the native state in the free energy coordinate.

Table III. *Determination of parameters of equilibrium urea unfolding of different systems in absence and presence of 500 mM NaCl at 25°C*

System	ΔG_1^0	m_1	ΔG_2^0	m_2	ΔG^0
	kJ/mol	*kJ/mol*	*kJ/mol*	*kJ/mol*	*kJ/mol*
OsINO1	6.4 ± 0.46	2.89 ± 0.24	28.85 ± 3.33	7.98 ± 0.84	32.25
PcINO1	9.0 ± 0.78	2.8 ± 0.19	16.9 ± 1.47	5.33 ± 0.46	25.9
ΔPcINO1.2	8.63 ± 0.43	2.75 ± 0.28	22.85 ± 2.55	6.5 ± 0.7	31.48
Os::PcINO1	6.3 ± 0.85	6.64 ± 1.13	17.8 ± 1.56	10.12 ± 1.37	24.1
OsINO1 + 500 mM NaCl	5.94 ± 0.643	2.07 ± 0.32	25.24 ± 4.62	6.0 ± 0.18	31.18
PcINO1 + 500 mM NaCl	8.9 ± 0.71	3.12 ± 0.441	23.69 ± 3.72	7.19 ± 0.11	32.59
ΔPcINO1.2 + 500 mM NaCl	7.94 ± 0.58	2.14 ± 0.34	23.74 ± 3.54	6.0 ± 0.086	31.68
Os::PcINO1 + 500 mM NaCl	8.4 ± 0.521	2.61 ± 0.33	21.0 ± 3.07	5.4 ± 0.078	29.4

It is therefore likely to assume that these intermediates have very native-like structures. The stability (ΔG^0) of these proteins were found to be quite different from each other in absence of salt but the difference diminished somewhat in presence of 500 mM NaCl. It was found that in absence of salt, removal of 37-amino acid residue stretch from PcINO1 changed the ΔG^0 from 25.9 kJ/mol for PcINO1 to 31.48 kJ/mol for ΔPcINO1.2, leading to stabilization by 5.58 kJ/mol. In other words the presence of this 37-amino acid residue stretch in PcINO1 has a structure-destabilizing effect. When the same 37-amino acid residue stretch of PcINO1 replaced the corresponding 37-amino acid residue stretch of OsINO1 resulting in Os::PcINO1, its stability was found to decrease from 32.25 to 24.1 kJ/mol. Thus it can be said that arrangement of residues in this stretch is such that it reduces protein stability in absence of NaCl. However, both the PcINO1 and Os::PcINO1 containing this 37-amino acid residue stretch when taken from no salt to high salt situation gained extra stability of 6.69 and 5.3 kJ/mol, respectively. Contrary to this, the other two proteins (ΔPcINO1.2 and OsINO1) that do not contain this 37-amino acid residue stretch either showed no extra stability or decreased stability when taken from no salt to high salt condition.

Modeling Study

In an attempt to construct three-dimensional models of OsINO1 and PcINO1 proteins, sequence similarity search was carried out by BLAST (Altschul et al., 1997) against MIPS proteins whose crystal structures have been deposited in the Protein Data Bank (PDB). Figure 10A shows the multiple sequence alignment done by ClustalW (Thompson et al., 1994) of PcINO1, OsINO1, and the yeast MIPS (ScINO1) for which the crystal structure (PDB ID 1P1J; Jin and Geiger, 2003) has been obtained. Sequence similarity between OsINO1 and PcINO1 is approximately 83%, whereas the same between OsINO1 and template and between PcINO1 and template are approximately 60% and 50%, respectively. Comparison of the 37-amino acid residue stretch of OsINO1 and PcINO1 revealed that there are 21 hydrophobic residues in OsINO1 compared to 15 in PcINO1. While these residues remained scattered in the stretch of PcINO1, they were found to be distinctly clustered in two stretches of eight and four residues in OsINO1 (Fig. 10B). The three-dimensional models of monomer for both OsINO1 and PcINO1 have been depicted in Figure 10, C and D. C_α backbone of homology-modeled PcINO1 and OsINO1 were superimposed separately on the C_α backbone of the yeast MIPS crystal structure. The pairwise root mean fits were 1.05 A^0 and 1.1 A^0, respectively, indicating that both the structures are essentially the same. In homology-modeled structures this 37-amino acid residue long stretch was mostly found to be in the loop region for both the proteins. More accurately the stretch corresponding to residues 174 to 206 is in the loop followed by a helix containing the rest of the stretch

(residues 206–210; Fig. 10, C and D). Furthermore, there are a number of well-distributed Ser and Thr in the 37-amino acid residue loop stretch of PcINO1 than OsINO1, which are the potential candidates for well-connected hydrogen bond network. Such four distinct hydrogen bonds made by Ser and Thr in PcINO1 have been presented in Table IV and shown in the ball-n-stick model (Fig. 10E). Moreover, when electrostatic potential of each residue from 174 to 210 of both PcINO1 and OsINO1 were plotted against the residue number, a distinct difference with respect to their surface electrostatic potential over this stretch was found (Fig. 11), where influence of charged environment was found to be greater over the stretch of PcINO1.

DISCUSSION

Stability of native folds of proteins and its response to changes in their environment both under in vitro as well as in vivo conditions has been a subject of intense study over the past several years (Jaenicke and Zavodszky, 1990; Jaenicke, 1991; Taneja and Ahmad, 1994; Murphy, 1995; Jaenicke and Bohm, 1998; Nelson and Onuchic, 1998). Since it is imperative for any protein to retain its functional integrity under changing environment, an insight into the mechanism through which functional proteins may achieve such potential constitutes an important area of investigation. An area of considerable interest in this direction has been generation of transgenic plants for acquisition of a stress-tolerant phenotype against major environmental stress by introgression of genes for such proteins, which function as stress-tolerant determinants (Hasegawa et al., 2000). Our previous work on a salt-tolerant MIPS from *Porteresia coarctata* (*PcINO1*) demonstrated that it is a variant of the *OsINO1* gene isolated from the domesticated rice *Oryza sativa*, being different in a 37-amino acid residue stretch (residues Trp-174 to Ser-210), and can characteristically synthesize the osmolyte inositol even under salt stress (Majee et al., 2004). This points toward an adaptational feature in MIPS protein evolution across diverse taxa for a specialized function similar to the archaeal MIPS that is functionally active only at high temperature (Chen et al., 2000). In this study we have established that the 37-amino acid stretch of PcINO1 is primarily responsible for its salt-tolerance property through the biochemical and biophysical characterization of in vitro generated mutants.

Characteristics of the in Vitro Generated PcINO1 Mutants and Hybrid Proteins vis à vis Salt Tolerance

Results presented herein clearly demonstrate that in addition to the loss of salt tolerance by deletion of the 37-amino acid residue stretch in ΔPcINO1.2 reported earlier (Majee et al., 2004), replacement of the corresponding 37-amino acid residue stretch in OsINO1 with the designated 37-amino acid residue stretch of
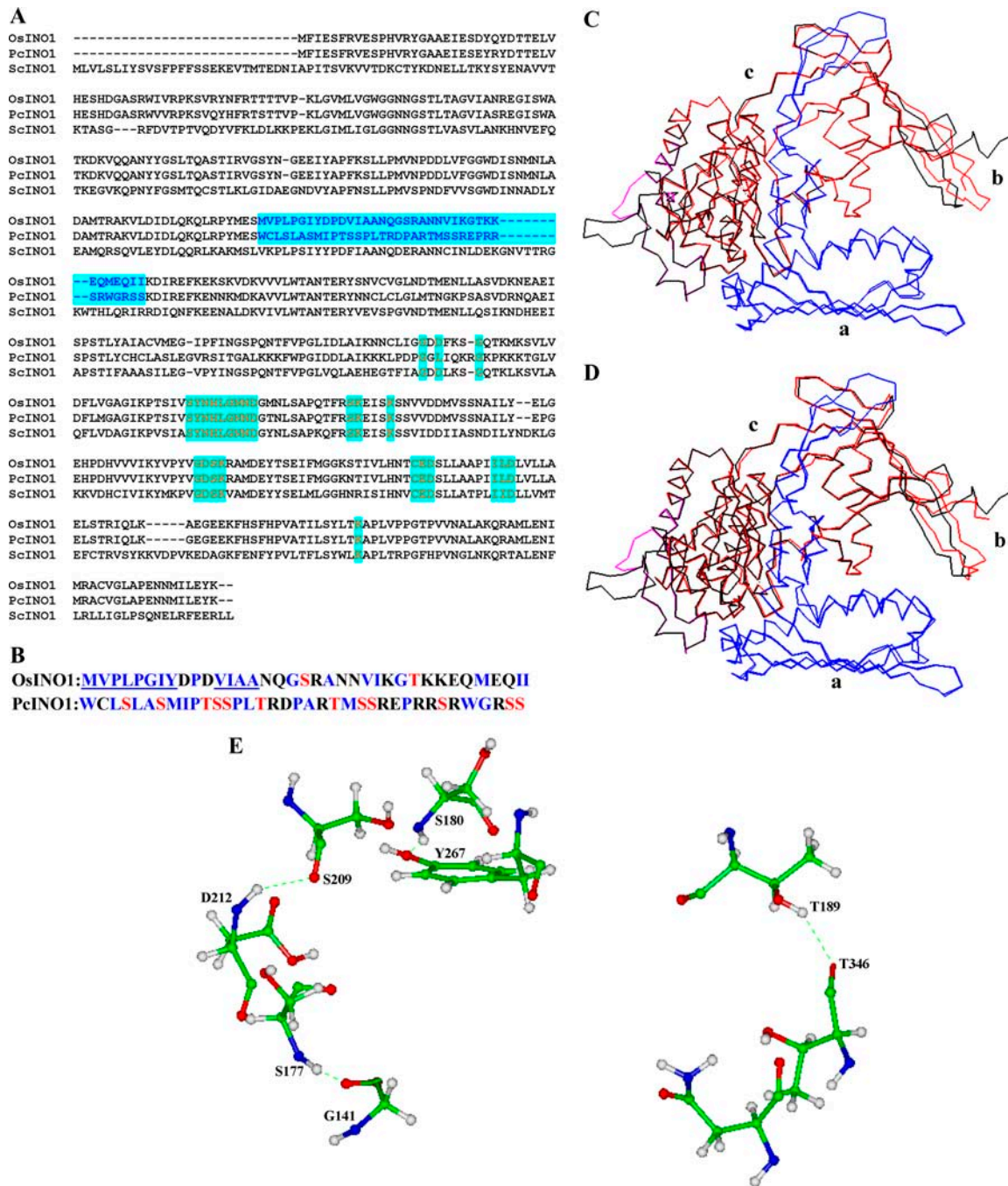
Figure 10. Sequence alignment and modeling studies. A, Multiple sequence alignment of amino acids in OsINO1, PcINO1, and ScINO1. The 37-amino acid stretch is shown in blue. The conserved amino acid residues or stretches belonging to the core catalytic region are shown in red. B, Difference in the amino acid composition in the 37-amino acid residue stretch of OsINO1 and PcINO1. Hydrophobic residues of both OsINO1 and PcINO1 are marked blue. The hydrophobic stretches in OsINO1 are underlined. Ser and Thr residues are marked in red. C, C$_\alpha$ backbone superimposition of homology-modeled OsINO1 on yeast MIPS crystal. D, C$_\alpha$ backbone superimposition of homology-modeled PcINO1 on yeast MIPS crystal. The C$_\alpha$ backbone of yeast MIPS crystal is shown in black. The C$_\alpha$ backbones of OsINO1 and PcINO1 are shown in red. The 37-amino acid residue stretch is shown in cayan and the catalytic domain is shown in blue. a, Tetramerization/catalytic domain; b, central domain; and c, Rossmann fold domain. E, The four distinct hydrogen bond networks mediated by Ser and Thr in PcINO1 shown in ball-n-stick model.

Table IV. *Ser- and Thr-mediated hydrogen bond network in PcINO1*

System PcINO1		Distance (A⁰)	Angle
Donor	Acceptor		
T_{189} (HG1; loop)	T_{346} (O; helix L)	2.25	145.61
S_{180} (HN) (loop)	Y_{267} (OH; helix H)	1.96	148.75
S_{209} (O; helix F)	D_{212} (HN; helix F)	2.08	141.85
S_{177} (HN; loop)	G_{141} (O; sheet S7)	1.88	166.77

PcINO1 resulted in attainment of a salt-tolerant property in the hybrid enzyme Os::PcINO1 (Fig. 4F). We have also tested the potential of this 37-amino acid residue peptide in conferring salt-tolerance characteristics to a MIPS from a heterologous source like *Brassica juncea*. The MIPS activity of recombinant purified protein from the *Brassica juncea* (BjINO1) that shares about 80% to 90% sequence homology with either OsINO1 or PcINO1, was found to be sensitive to increasing concentration of NaCl in vitro like OsINO1; however, when the corresponding 37-amino acid residue stretch of BjINO1 was replaced by the same of PcINO1, generating Bj::PcINO1 hybrid, the in vitro MIPS activity was found to be tolerant to increasing concentration of NaCl, like PcINO1 and Os::PcINO1 hybrid (Fig. 4F). Like ΔPcINO1.2 and Os::PcINO1, functional viability of BjINO1 and Bj::PcINO1 were also tested through functional complementation assay (data not shown). Our in vivo functional complementation experiment, in line with the in vitro synthase activity, where the deletion and both the hybrid proteins showed almost equal activity like wild enzymes (Fig. 4E), suggests that either the deletion or the substitution of this 37-amino acid residue stretch resulting in ΔPcINO1.2 and Os::PcINO1 or Bj::PcINO1, respectively, retained the catalytic structure of the active site as opposed to ΔPcINO1.1 in which a part of the core catalytic region (Majumder et al., 2003) was deleted. Hence although not directly involved in the catalysis, this 37-amino acid residue stretch of PcINO1 may control either the access of the substrate to the catalytic site or alter the geometric arrangement around it to alter substrate-binding properties in presence of high salt.

To find out how the mutant proteins differ with respect to their kinetic properties, we also compared K_{m}, V_{max} of purified ΔPcINO1.2 and Os::PcINO1, along with that of OsINO1 and PcINO1 (Table I). The K_{m} for NAD⁺ of ΔPcINO1.2, being the highest of all four, has been found to be 2.4 and 2.7 times that of OsINO1 and PcINO1, respectively, suggesting a decrease in the affinity of the enzyme toward NAD⁺ binding. However, the K_{m} for the same of Os::PcINO1 was found to be 1.5 times lower than that of ΔPcINO1.2, which suggests an increase in the NAD⁺ affinity. From the sequence analysis in light of the available yeast MIPS crystal structure (Stein and Geiger, 2002; Jin and Geiger, 2003) it has been found that the 37-amino acid residue stretch in PcINO1 seems to be an insertion over the Rossmann fold. So the above result points toward the possibility of perturbation in the NAD⁺

binding in presence of salt and the 37-amino acid stretch of PcINO1 may somehow control the binding of NAD⁺ to the enzyme.

Distinct differences in the in vivo salt-tolerance property of the different PcINO1 mutants were observed when *S. pombe* transformed with *PcINO1*, *OsINO1*, *ΔPcINO1.2*, and *Os::PcINO1* and were allowed to grow in presence of increasing concentration of NaCl on solid media (Fig. 3, A–F). Our choice for this purpose was *S. pombe* over *S. cerevisiae* since the former, being a natural inositol auxotroph, presents an excellent model to elucidate the phenotypic expression of the *INO1* gene and to study the effect of the mutation in the *PcINO1* gene on growth of the organism in presence of salt. Growth of *PcINO1*- and *Os::PcINO1*-transformed *S. pombe* even under salt stress as opposed to *OsINO1* and *ΔPcINO1.2*, clearly indicates the salt-induced inhibition of enzyme activity lacking the 37-amino acid residue stretch of PcINO1 as opposed to enzymes containing the same, which remain active in vivo even in presence of high salt. This probably ensures the unabated production of inositol in the *PcINO1*- and *Os::PcINO1*-transformed cells that protect them from deleterious salt effects as opposed to *OsINO1*- and *ΔPcINO1.2*-transformed cells. Similar results were obtained in liquid cultures also and the functional expression of these gene products in both cases was confirmed through western-blot analysis (data not shown).

Fluorescence and CD-Based Studies

The Trp fluorescence-quenching experiments revealed that the structures of OsINO1 and PcINO1, particularly around the Trp residues, were affected differentially by salt. OsINO1 has five Trp and PcINO1 has eight, all being located primarily in the N-terminal region in both, the first four Trp residues being located at identical position. The 37-amino acid residue stretch of PcINO1 contains two more surface-exposed Trp-174 and Trp-206, followed by two less exposed Trp-229
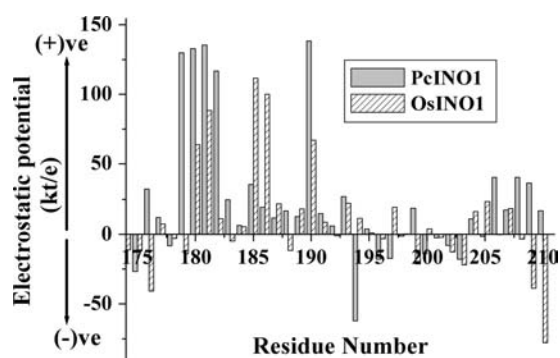
Figure 11. Distribution of electrostatic potential across the 37-amino acid residue stretch. Bar diagram of electrostatic potential of each residue from 174 to 210 of OsINO1 and PcINO1 in the 37-amino acid residue stretch.

and Trp-289 as indicated from modeling studies; the corresponding region of OsINO1 having only one buried Trp-229. Since the surface-exposed Trps do not contribute much to the Trp fluorescence intensity because of their low quantum yield, the intensity-contributing Trps are those away from this loop region. Quenching of Trp fluorescence either of OsINO1 (Majee et al., 2004) or ΔPcINO1.2 indicated that salt alters the conformation of both in such a way as to bring some of the buried Trps close to the surface, enhancing the collisional quenching, or by an alternative mechanism of enhanced energy transfer due to proximal redistribution of Trp neighboring groups, whose polarity remained unchanged. A change in secondary structure at high salt concentration was also reflected in the CD data (Fig. 8, B and C). On the other hand, both PcINO1 and Os::PcINO1 are able to maintain their structural rigidity in presence of salt, disallowing the Trp positions to be changed much from those in absence of salt. Lack of change in the internal fold of both PcINO1 and Os::PcINO1 is also indicated by the CD spectra, whose nature qualitatively remained unchanged in presence of salt (Fig. 8, A and D).

Surface Hydrophobicity as an Index of Salt Sensitivity versus Salt Tolerance

The effect of this 37-amino acid residue stretch on the salt-induced structural plasticity or rigidity is directly provided by the highly sensitive bis-ANS binding results (Table II) that reflect that the presence of this stretch in PcINO1 and Os::PcINO1 caused minimal changes in the surface exposure of the hydrophobic pockets on increasing salt concentration but its absence in OsINO1 and ΔPcINO1.2 led to a large increase in the surface exposure of hydrophobic residues (Fig. 6A). The presence of 21 hydrophobic residues in clusters in OsINO1 compared to 15 scattered of such in PcINO1 (Fig. 10B) generally explains the higher surface hydrophobicity of OsINO1 over PcINO1 in absence of salt. The excess exposure of the hydrophobic clefts in presence of salt in the cases of OsINO1 and ΔPcINO1.2 makes them susceptible to aggregation (Fig. 7A) as opposed to either PcINO1 or Os::PcINO1, which are resistant to such salt-induced aggregation (Fig. 7B). It may be interesting to point out here that CD data in presence of 500 mM NaCl of OsINO1 and ΔPcINO1.2 points to some increase in β-sheet structure at the expense of helix structure. Since salts screen the electrostatic interactions on the protein surface, the hydrophobic interactions are screened through protein oligomerization interaction (Biswas et al., 2002). Hence, loss of MIPS activity may be directly related to this oligomerization. Further, the salt-induced surface hydrophobic exposure is accompanied also by rearrangements of internally buried groups, the loss of enzymatic function may also be due to both restructuring of the catalytic site and physical blocking of the access path of the substrate by oligomerization.

It has also been noted that there are a good number of well-distributed Sers and Thrs in PcINO1 than OsINO1 particularly in the 37-amino acid residue loop stretch (Fig. 10, B and E). These residues form four well-connected salt bridge networks with the neighboring residues, both within and outside the loop region (Table IV) that contributes to salt stability in PcINO1 and the Os::PcINO1. Since such an extensive salt bridge is not possible in OsINO1, screening of surface electrostatic interactions in presence of salt somewhat destabilizes OsINO1, leading to structural reorganization. Furthermore, as distribution of electrostatic potential is purely context dependent, it was observed that the charge distribution over this stretch of PcINO1 varies considerably from positive to negative with a greater positive potential, whereas in the case of OsINO1 almost a uniform but less charge distribution is observed. This possibly accounts for the higher surface polarity over the 37-amino acid residue stretch of PcINO1, which in turn can be screened out by the salt ions and thus protects the enzyme from the salt-induced inactivation as opposed to OsINO1.

Assessment of Thermodynamic Stability in the Absence and Presence of Salt

There are plenty of indications from the above discussion that the salt affects the stability of OsINO1 and PcINO1 differently, as indicated further by the urea denaturation study (Table III). Both PcINO1 and the Os::PcINO1 were found to be stabilized in presence of salt, resulting in a $\Delta\Delta G_s^0$ ($=\Delta G_{salt}^0 - \Delta G_{no\ salt}^0$) of 6.69 and 5.3 kJ/mol. OsINO1 was destabilized as $\Delta\Delta G_s^0$ and is -1.07 kJ/mol, the minus sign indicating destabilization. ΔPcINO1.2 on the other hand did not gain additional stability in presence of salt, as the $\Delta\Delta G_s^0$ is nearly zero. This suggests that the existence of the loop region reflects upon the thermodynamic differences in presence of salt more prominently. Interestingly, in absence of salt, existence of the loop sequence of PcINO1 has a destabilizing effect compared to ΔPcINO1.2, as $\Delta\Delta G_{37P}^0$ (defined as $\Delta G_{PcINO1}^0 - \Delta G_{\Delta PcINO1.2}^0$) is -5.58 kJ/mol. On the contrary, the loop sequence of OsINO1 contributes to protein stability in absence of salt, as $\Delta\Delta G_{37R}^0$ ($=\Delta G_{OsINO1}^0 - \Delta G_{\Delta PcINO1.2}^0$) is $+0.77$ kJ/mol. Because of the two opposing free energy contributions of the two 37-amino acid residue loop stretches of OsINO1 and PcINO1 in absence of salt, the replacement of OsINO1 stretch by that of PcINO1 from simple thermodynamic additivity assumption is predicted to result in loss of stability by 6.35 kJ/mol ($=-5.58 - 0.77$ kJ/mol). Indeed the Os::PcINO1 was found to have the thermodynamic stability lower than that of OsINO1 by 8.15 kJ/mol from 32.25 to 24.1 kJ/mol. Considering the simple assumption and analysis, this qualitative agreement is quite significant in accordance with the position of chloride anion as a destabilizer in the Hofmeister series of kosmotropes and chaotropes (Elcock and McCammon, 1998; Dominy et al., 2002; Apetri and Surewicz, 2003).

The destabilization of OsINO1 in presence of NaCl may be considered as a typical and mildly chaotropic effect. The stabilizing effect of NaCl on PcINO1 and the Os::PcINO1 represents atypical salt effects (Apetri and Surewicz, 2003). This sequence-dependent difference in salt effect may arise from formation and disruption of salt bridges, which are nothing but strong hydrogen bonds (Strop and Mayo, 2000; Bosshard et al., 2004) formed between two closely spaced interacting polar or charged residues (Table IV). Energy contribution toward stability of proteins for the salt bridge formation is usually low (about 4.0 kJ/mol) and the stabilization energy is contributed mainly from the increase in entropy of the solvent compensated by the energy required to break the hydrogen bond with water (Stigler, 1991; Strop and Mayo, 2000). The stabilization of PcINO1 and the Os::PcINO1 in the presence of salt by 5.3 to 6.69 kJ/mol lends strong support in favor of the salt bridge formation.

A comparable example is found in the allene oxide cyclase gene from *Bruguiera sexangula* wherein a 70-amino acid stretch has been identified as the salt-tolerance determinant of the gene product (Yamada et al., 2002). Designated as mangrin, this gene is reported to be capable of conferring salt tolerance when introgressed to a number of pro- and eukaryotic systems (Yamada et al., 2002), a characteristic also shared by *PcINO1* (A. Das-Chatterjee, L. Goswami, S. Maitra, K. Ghosh Dastidar, S. Roy, B. Das, M. Majee, S. Bhattacharyya, S. Pattnaik, and A.L. Majumder, unpublished data). In addition to the identification of the 37-amino acid residue stretch as the salt-tolerance determinant in PcINO1, we have been able to demonstrate that this stretch can also attribute salt-tolerance property to an otherwise salt-sensitive MIPS by replacement of the corresponding amino acid stretch. Such recombination has resulted in salt tolerance of Os::PcINO1 or Bj::PcINO1 hybrid gene products. Since the MIPS gene sequences of plants are fairly conserved (Majumder et al., 2003), it is conceivable that any plant MIPS may thus be made salt tolerant by similar protein engineering strategies.

MATERIALS AND METHODS

Reagents

D-Glc-6-P (disodium salt), nicotinamide adenine dinucleotide (disodium salt; NAD+), phenylmethylsulfonyl fluoride, isopropyl thiogalactoside, 5′ bromo 4-chloro 3-indolyl D-galactopyranoside, bis-ANS, and β-mercaptoethanol (β-ME) were purchased from Sigma. All column chromatographic materials were purchased from Amersham Pharmacia and Bio-Rad. All restriction enzymes, T4 DNA ligase, and RNase were purchased from New England Biolabs. PCR reagents, oligonucleotides, Hifi Taq polymerase, and pGEMT-Easy vector were purchased from GIBCO-BRL and Promega. All other chemicals used were of analytical reagent grade purity unless otherwise specified.

Generation and Molecular Cloning of Mutant and Hybrid Clones of PcINO1

Two *PcINO1* mutants, namely ΔPcINO1.1 and ΔPcINO1.2 were generated by PCR as described earlier (Fig. 1B; Majee et al., 2004). Since both *OsINO1* and

PcINO1 contain one unique *Pst*I and one unique *Eco*RV site at the same position, the OsINO1/PcINO1 hybrid termed *Os::PcINO1* was generated simply by replacing a 5′-3′ *Pst*I-*Eco*RV fragment of *OsINO1* with the same fragment from *PcINO1* through restriction digestion (Fig. 1C).The second hybrid gene between Brassica MIPS and *PcINO1* (termed as Bj::PcINO1) was generated by substituting the corresponding 37-amino acid residue stretch of BjINO1 with that of PcINO1 by PCR using the following primers: P1, 5′-acatatgttcatcgagagcttccg-3′; P2, 5′-ggagctcgttctccatgtaaggcctga-3′; P3, 5′-aggtaccaaggacatgagggagttt-aag-3′; P4, 5′-gctcgagcttgttactccaggatcatgt-3′; P5, 5′-atcgagctctggtgcctctccctggcatctatg-3′; and P6, 5′-cggggtacctgatgatctgccccatctgctcctt-3′ (Fig. 1D). INO1 from *Brassica juncea* (henceforth termed BjINO1) was PCR amplified by using primers based on the *Brassica napus* INO1 gene (U66307) following the protocol for isolating OsINO1/PcINO1 (Majee et al., 2004). All the genes (wild, mutant, and hybrids) were finally cloned into pET-20b(+) expression vector (Novagen) at *Nde*I and *Xho*I sites and mutations were confirmed by sequencing from University of Delhi, South campus, India.

Funtional Complementation of ΔPcINO1.1, ΔPcINO1.2, and Os::PcINO1 in Yeast FY250 (MATα trp1 his3 ura3 leu2 Ino1::HIS3) Inositol Auxotrophic Strain

A yeast (*Saccharomyces cerevisiae*)-based functional complementation assay for the confirmation of the MIPS activity of the mutant and hybrid gene products was performed as per procedure described in detail earlier (Chatterjee et al., 2004; Majee et al., 2004).

Expression of Wild and Mutant INO1 Genes in *Schizosaccharomyces pombe* (h⁻ leu1-32 ura4-D18) PR109

OsINO1, *PcINO1*, ΔPcINO1.2, and *Os::PcINO1* were subcloned downstream of a thiamine repressible, *nmt* promoter in a yeast binary expression vector *pREP1* (Maundrell, 1993). pGEMT-Easy vector (Promega) harboring all the above-mentioned genes was digested with *Nde*I and *Xho*I. The digested products were then directionally ligated to pERP1 at *Nde*I and *Sal*I sites using T4 DNA ligase. Positive clones were checked by digestion with *Nde*I and *Sma*I. All pREP1 constructs harboring different mutant and wild-type genes were transformed in *S. pombe* cells according to the protocol described by Chaudhuri et al. (1997).

For growth experiments, transformed *S. pombe* cells were allowed to grow in complete solid synthetic Edinburgh minimal medium (EMM; Alfa et al., 1992) supplemented with 2 μM inositol and containing different NaCl concentrations (0–500 mM). For this purpose first *PcINO1*, *OsINO1*, ΔPcINO1.2, *Os::PcINO1*, and pREP1 transformed *S. pombe* cells were grown in EMM broth supplemented with 2 μM inositol at 30°C until the A_{600} reached between 0.6 to 0.7. Then, equal numbers of cells were plated onto solid EMM media supplemented with 2 μM inositol and increasing NaCl concentration as stated above. Plates were incubated at 30°C for 48 h.

Bacterial Overexpression and Purification of the Recombinant Proteins

Bacterial overexpression of all mutant or hybrid genes (ΔPcINO1.1, ΔPcINO1.2, Os::PcINO1, BjINO1, and Bj::PcINO1), recovery of the expressed recombinant proteins from the particulate fraction, and their subsequent purification along with the wild type were carried out essentially by following the procedure described earlier (Majee et al., 2004). After the final purification, all proteins were extensively dialyzed against 20 mM Tris-HCl (pH 7.5), 10 mM NH₄Cl, 10 mM β-ME, and 20% glycerol concentrated and stored at −20°C for further use.

Assay of MIPS

MIPS assay was done colorimetrically by the periodate oxidation method of Barnett et al. (1970) and further corroborated by the inositol-1-P phosphatase assay described by RayChaudhuri et al. (1997). The amount of inorganic phosphate liberated from the MIPS reaction product either by periodate oxidation or inositol 1-P phosphatase reaction was estimated by the method of Chen et al. (1956).

Estimation of Protein

Protein was estimated according to the method of Bradford (1976) with the Bio-Rad protein assay kit using bovine serum albumin as a standard.

Analytical SDS-PAGE and Western Blotting

Ten-percent SDS-PAGE was performed according to Laemmli (1970). Immunodetection and proteins were done as described by Chatterjee et al. (2004).

Trp Fluorescence Quenching in the Presence and Absence of NaCl

Purified ΔPcINO1.2, Os::PcINO1, and OsINO1 and PcINO1 (serving as controls) were separately dialyzed against 1 L buffer (20 mM Tris-HCl, pH 7.5, and 10 mM β-ME) with two changes overnight at 4°C. Nine-hundred microliters of approximately 170 μg/mL of both the proteins were used in a total 1 mL reaction mixture in a quartz cuvette (4 mm × 4 mm). In both cases proteins were incubated at 37°C as well as at 25°C for 10 min both in absence as well as in presence of different concentrations of NaCl (100–600 mM). Excitation wavelength was selected at 295 nm and the emission was scanned at a speed of 240 nm/min from 310 to 400 nm using excitation and emission slit width of 5.0 nm each. Each spectrum was an average of three scans. Appropriate control buffer spectra were subtracted from sample spectra to generate the fluorescence spectra of the proteins. Wavelength of maximum emission for each spectrum was determined by derivative analysis using the instrument software.

Bis-ANS Binding Study

Each purified protein was extensively dialyzed against (20 mM Tris-HCl, pH 7.5, and 10 mM β-ME) at 4°C. In each case 1 mL of approximately 50 μg/mL dialyzed protein was first incubated at 37°C for 10 min in absence or presence of 500 mM NaCl and then titrated with aqueous solution of bis-ANS (300 μM) in total 1 mL reaction volume at room temperature. In each case bis-ANS was added in small aliquots (2, 4, 8, and 10 μL and so on until saturation) to the protein solution, mixed well, and incubated for 1 min. Emission was recorded at 490 nm after exciting the samples at 390 nm, using excitation and emission slit width of 5.0 nm each. Binding isotherms were generated by plotting fluorescence intensity (F) at 490 nm against the wavelength values. To determine the stoichiometry (n) and dissociation constant (k_d) of these binding phenomena, reverse bis-ANS titration was done. In this case 1 mL of 0.1 μM bis-ANS solution was titrated by adding small aliquots (each 10 μL) of protein (approximately 450 μg/mL), which was preincubated at 37°C for 10 min with and without 500 mM NaCl. After each addition, the solution was mixed well and kept at room temperature for 1 min.

Aggregation Assay in the Presence and Absence of NaCl

Purified ΔPcINO1.2, Os::PcINO1, and OsINO1 and PcINO1 (serving as controls) were dialyzed separately in 1 L of buffer (20 mM Tris-HCl, pH 7.5, and 10 mM β-ME) overnight at 4°C. Nine-hundred microliters of approximately 350 μg/mL of each protein was subjected to static light scattering at 360 nm in absence and presence of different concentrations of increasing NaCl (100–500 mM) in total 1 mL reaction volume at 37°C in SHIMADZU UV-160A for up to 170 min following the protocol described by Horwitz (1992). Optical density of the samples at 360 nm was measured over a period of 170 min at regular intervals where increased absorbance was indicative of aggregation of the protein samples.

CD Spectroscopy in the Presence and Absence of NaCl

Protein samples were dialyzed separately against 1 L of filter-sterilized 5 mM sodium phosphate buffer, pH 7.6, with three changes overnight at 4°C. Far-UV CD spectroscopy was done with 1.350 mL of approximately 100 μg/mL recombinant purified OsINO1, PcINO1, ΔPcINO1.2, and Os::PcINO1 in a total 1.5 mL reaction volume in absence and presence of increasing concentration of NaCl (100–500 mM) at room temperature. In both the cases proteins were preincubated at 37°C for 10 min both in absence as well as in presence of different concentrations of NaCl. An average of five scans was recorded at 0.2 step resolution, 10 nm/min scan speed, 1.0 nm band width, and 2 s time

constant in a Jasco600 spectrophotopolarimeter. Data were processed by several secondary structure analysis programs such as SELCON3, CONTIN, CDSSTR, and CDNN, available on the Web.

Urea Unfolding Equilibrium in the Absence and Presence of 500 mM NaCl

Urea unfolding equilibrium was carried out spectroflurometrically in a Hitachi-F-4500 spectrofluorimeter with all four purified enzymes under identical conditions in absence and presence of 500 mM NaCl at room temperature (approximately 25°C). In each case approximately 50 μg of protein, which was extensively dialyzed against 20 mM Tris-HCl (pH 7.5), 10 mM β-ME, and 5% glycerol for approximately 16 h at 4°C, was preincubated with 0 to 8 M (in total 13 sets) urea in total 1 mL reaction mixture in absence or in presence of 500 mM NaCl at room temperature (approximately 25°C) for almost 16 h. Emission spectra were recorded in a quartz cuvette (4 mm × 4 mm) by scanning from 300 to 400 nm after excitation at 295 nm, using excitation and emission slit width of 5.0 nm each. Each spectrum was an average of three scans. Appropriate control buffer spectra were subtracted from each sample spectra for each set to generate the fluorescence spectra of the proteins at different concentrations of urea. Wavelength of maximum emission for each spectrum was determined by derivative analysis using the instrument software. Maximum intrinsic fluorescence intensity value for each spectrum was normalized by taking the ratio of intensity at 337 nm and intensity at 350 nm ($I_{337\,nm}/I_{350\,nm}$) using the instrument software. $I_{337\,nm}/I_{350\,nm}$ values were plotted against the urea concentration in each set for each enzyme. $C_{0.5}$ value for each set was determined by fitting the plot to sigmoidal curve using Microcal Origin 6.0.

Modeling Study of OsINO1 and PcINO1

The amino acid sequences of PcINO1 and OsINO1 were taken from GenBank (accession nos. for PcINO1: AAP74579 and OsINO1: BAA25729). The atomic coordinate of yeast MIPS complexed with NADH (PDB code: 1P1J; Jin and Geiger, 2003) was obtained from the PDB (Berman et al., 2000). The chain A of this x-ray structure was used as the template to build the three-dimensional models of OsINO1 and PcINO1 using the program MODELLER (Sali and Blundell, 1993). Energy minimization of both the models were carried out by conjugate gradient method using the Consistent Valence Force Field (Hagler et al., 1979) of the Discover program (Insight II, BIOSYM/MSI, 1995) until all the structures reached the final derivative of the 0.0042 kJ/mol. The stereochemical quality of the models was checked using the program PROCHECK (Laskovski et al., 1993) and Ramachandran plots (Ramachandran and Sashisekharan, 1968) were drawn for both the models, according to which no residue was present in the disallowed region for both the models. Programs MODELLER and PROCHECK were run on a Silicon Graphics O2 R12000 workstation. The visualization of the above studies was done using the program InsightII (Insight II, BIOSYM/MSI, 1995).

Electrostatic potential was calculated using the program DELPHI (Insight II, BIOSYM/MSI, 1995) implemented in InsightII solving a finite difference solution to the nonlinear Poisson-Boltzmann equation. Dielectric constants of 80.0 and 2.0 were used for solvent and solute, respectively. The ionic strength of the solvent was 0.145 M.

LITERATURE CITED

Albany JR (2004) Structure and Dynamics of Macromolecules: Absorption and Fluorescence Studies. Elsevier, St. Louis

Alfa C, Fantes P, Hyams J, McLeod M, Warbrick E (1992) Experiments with Fission Yeast: A Laboratory Manual. Cold Spring Harbor Laboratory Press, Cold Spring Harbor, NY

Altschul SF, Madden TL, Schaffer AA, Zhang J, Zhang Z, Miller W, Lipman D (1997) Gapped BLAST and PSI-BLAST: a new generation of protein database search programs. Nucleic Acids Res 25: 3389–3402

Apetri AC, Surewicz WK (2003) Atypical effect of salts on the thermodynamic stability of human prion protein. J Biol Chem 278: 22187–22192

Barnett JEG, Brice RE, Corina DL (1970) A colorimetric determination of inositol monophosphatase as an assay for D glucose-6- phosphate 1-L- myo-inositol 1 phosphate cyclase. Biochem J 119: 183–186

Berman MH, Westbrook J, Feng J, Gillilang G, Bhat TN, Weissig H, Sindyalov IN, Bourne PE (2000) The protein data bank. Nucleic Acids Res 28: 235–242

Biswas A, Das KP (2004) Role of ATP on the interaction of alpha-crystallin with its substrates and its implications for the molecular chaperone function. J Biol Chem 279: 42648–42657

Biswas A, Saha S, Das KP (2002) Structural features of molecular chaperons: a possible micellar connection. J Surface Sci Technol 18: 1–24

Biswas BB, Ghosh B, Majumder AL (1984) myo-Inositol polyphosphates and their role in cellular metabolism: a proposed cycle involving glucose-6-phosphate and myo-inositol phosphates. Subcell Biochem 10: 237–280

Bohnert HJ, Nelson DE, Jensen RG (1995) Adaptations to environmental stresses. Plant Cell 7: 1099–1111

Bosshard HR, Marti DN, Jelesarov I (2004) Protein stabilization by salt bridges: concepts, experimental approaches and clarification of some misunderstandings. J Mol Recognit 17: 1–16

Bradford MW (1976) Quantitation of microgram quantities of protein utilizing the principle of protein dye binding. Anal Biochem 72: 248–254

Cardamone M, Puri BR (1992) Spectrofluorimetric assessment of the surface hydrophobicity of proteins. Biochem J 282: 589–593

Chatterjee A, Majee M, Ghosh S, Majumder AL (2004) sll1722, an unassigned ORF of Synechocystis PCC 6803, codes for L-myo-inositol 1-phosphate synthase. Planta 218: 989–998

Chaudhuri B, Ingavale S, Bachhawat AK (1997) apd1+, a gene required for red pigment formation in ade6 mutants of Schizosaccharomyces pombe, encodes an enzyme required for glutathione biosynthesis: a role for glutathione and a glutathione-conjugate pump. Genetics 145: 75–83

Chen L, Zhou C, Yang H, Roberts MF (2000) Inositol-1-phosphate synthase from Archaeoglobus fulgidus is a class II aldolase. Biochemistry 39: 12415–12423

Chen RS, Toribara TY, Warner H (1956) Microdetermination of phosphorus. Anal Chem 28: 1756–1758

Das BK, Bhattacharyya T, Roy S (1995) Characterization of a urea induced molten globule intermediate state of glutaminyl-tRNA synthetase from Escherichia coli. Biochemistry 34: 5242–5247

Das KP, Petrash J, Surewicz WK (1996) Conformational properties of substrate proteins bound to a molecular chaperone alpha-crystallin. J Biol Chem 271: 10449–10452

Das KP, Surewicz WK (1995) Temperature-induced exposure of hydrophobic surfaces and its effect on the chaperone activity of alpha-crystallin. FEBS Lett 369: 321–325

Dominy BN, Perl D, Schmid FX, Brooks CL III (2002) The effects of ionic strength on protein stability: the cold shock protein family. J Mol Biol 319: 541–554

Eftink MR, Ghiron CA (1981) Fluorescence quenching studies with proteins. Anal Biochem 114: 199–227

Elcock AH, McCammon JA (1998) Electrostatic contributions to the stability of halophilic proteins. J Mol Biol 280: 731–748

Fersht AR (1999) Structure and Mechanism in Protein Science: A Guide to Enzyme Catalysis and Protein Folding. Freeman and Company, New York

Hagler AT, Lifson S, Dauber P (1979) Consistent force field studies of intermolecular forces in hydrogen-bonded crystals. 2. A benchmark for the objective comparison of alternative force. J Am Chem Soc 101: 5122–5130

Hasegawa PM, Bressan RA, Zhu JK, Bohnert HJ (2000) Plant cellular and molecular responses to high salinity. Annu Rev Plant Physiol Plant Mol Biol 51: 463–499

Horowitz PM, Hua S, Gibbons DL (1995) Hydrophobic surfaces that are hidden in chaperonin Cpn60 can be exposed by formation of assembly-competent monomers or by ionic perturbation of the oligomer. J Biol Chem 270: 1535–1542

Horwitz J (1992) Alpha-crystallin can function as a molecular chaperone. Proc Natl Acad Sci USA 89: 10449–10453

Ingavale SS, Bachhawat AK (1999) Restoration of inositol prototrophy in the fission yeast Schizosaccharomyces pombe. Microbiology 145: 1903–1910

Ishitani M, Majumder AL, Bornhouser A, Michalowski CB, Jensen RG,

Bohnert HJ (1996) Coordinate transcriptional induction induction of myo-inositol metabolism during environmental stress. Plant J 9: 537–548

Jaenicke R (1991) Protein stability and molecular adaptation to extreme conditions. Eur J Biochem 202: 715–718

Jaenicke R, Bohm G (1998) The stability of proteins in extreme environments. Curr Opin Struct Biol 6: 738–748

Jaenicke R, Zavodszky P (1990) Protein under extreme physical conditions. FEBS Lett 268: 344–349

Jin X, Geiger JH (2003) Structure of NAD and NADH bound 1-L-myo-inositol 1-phosphate synthase. Acta Crystallogr D 59: 1154–1164

Kanter U, Usadel B, Guerineau F, Li Y, Pauly M, Tenhaken R (2005) The inositol oxygenase gene family of Arabidopsis is involved in the biosynthesis of nucleotide sugar precursors for cell-wall matrix polysaccharides. Planta 221: 243–254

Laemmli UK (1970) Cleavage of structural proteins during the assembly of bacteriophage T4. Nature 227: 680–685

Lakowicz JR (1983) Principles of Fluorescence Spectroscopy. Plenum Press, New York, pp 258–304

Laskovski RA, MacArthur MW, Moss DS, Thornton JM (1993) PROCHECK: a program to check the stereochemistry of protein structure. J Appl Crystallogr 26: 283–291

Loewus FA, Murthy PN (2000) myo-Inositol metabolism in plants. Plant Sci 150: 1–19

Lorence A, Chevone BI, Mendes P, Nessler CL (2004) myo-Inositol oxygenase offers a possible entry point into plant ascorbate biosynthesis. Plant Physiol 134: 1200–1205

Majee M, Maitra S, Ghosh Dastidar K, Pattnaik S, Chatterjee A, Hait NC, Das KP, Majumder AL (2004) A novel salt-tolerant L-myo-inositol-1-phosphate synthase from Porteresia coarctata (Roxb.) Tateoka, a halophytic wild rice. J Biol Chem 279: 28539–28552

Majumder AL, Chatterjee A, Ghosh Dastider K, Majee M (2003) Diversification and evolution of L-myo-inositol 1-phosphate synthase. FEBS Lett 533: 3–10

Maundrell K (1993) Thiamine-repressible expression vectors pREP and pRIP for fission yeast. Gene 123: 127–130

Mumberg D, Muller R, Funk M (1995) Yeast vectors for the controlled expression of heterologous proteins in different genetic backgrounds. Gene 156: 119–122

Murphy KP (1995) Non covalent forces important to the conformational stability of protein structures. In BA Shirley, ed, Protein Stability and Folding: Theory and Practice, Vol 40. Humana Press, Totowa, NJ, pp 1–34

Nelson ED, Onuchic JN (1998) Proposed mechanism for stability of proteins to evolutionary mutations. Proc Natl Acad Sci USA 95: 10682–10686

Nelson ED, Rammesmayer G, Bohnert HJ (1998) Regulation of cell specific inositol metabolism and transport in plant salinity tolerance. Plant Cell 10: 1211–1219

Ramachandran GN, Sashisekharan V (1968) Conformation of polypeptides and proteins. Adv Protein Chem 23: 238–283

RayChaudhuri A, Hait NC, DasGupta S, Bhaduri TJ, Deb R, Majumder AL (1997) L-myo-lnositol 1-phosphate synthase from plant sources (characteristics of the chloroplastic and cytosolic enzymes). Plant Physiol 115: 727–736

Sali A, Blundell TL (1993) Comparative protein modeling by satisfaction of spatial restraints. J Mol Biol 234: 779–815

Sambrook J, Fritsch EF, Maniatis T (1989) Molecular Cloning: A Laboratory Manual, Ed 2, Cold Spring Harbor Laboratory Press, Cold Spring Harbor, NY

Sheveleva E, Chmara W, Bohnert HJ, Jensen RG (1997) Increased salt and drought tolerance by D-ononitol production in transgenic Nicotiana tabaccum L. Plant Physiol 115: 1211–1219

Sreerama N (1993) A self-consistent method for the analysis of protein secondary structure from circular dichroism. Anal Biochem 209: 32–44

Sreerama N, Venyaminov SY, Woody RW (1999) Estimation of the number of alpha-helical and beta-strand segments in proteins using circular dichroism spectroscopy. Protein Sci 8: 370–380

Stein AJ, Geiger JH (2002) The crystal structure and mechanism of 1-L-myo-inositol-1-phosphate synthase. J Biol Chem 277: 9484–9491

Stigler DS (1991) Protein stability: electrostatics and compact denatured states. Proc Natl Acad Sci USA 88: 4176–4180

Strop P, Mayo SL (2000) Contribution of surface salt bridges to protein stability. Biochemistry 39: 1251–1255

Sun TX, Akhtar NJ, Liang JJN (1999) Thermodynamic stability of human lens recombinant alphaA- and alphaB-crystallins. J Biol Chem 274: 34067–34071

Taji T, Ohsumi C, Iuchi S, Seki M, Kasuga M, Kobayashi M, Yamaguchi-Shinozaki K, Shinozaki K (2002) Important roles of drought- and cold-inducible genes for galactinol synthase in stress tolerance in *Arabidopsis thaliana*. Plant J **29:** 417–426

Taneja S, Ahmad F (1994) Increased thermal stability of proteins in the presence of amino acids. Biochem J **303:** 147–153

Thompson JD, Higgins DG, Gibson TJ (1994) CLUSTAL W: improving the sensitivity of progressive multiple sequence alignment through sequence weighing, position-specific gap penalties and weight matrix choice. Nucleic Acids Res **22:** 4673–4680

Vernon DM, Bohnert HJ (1992) A novel methyl transferase induced by osmotic stress in the facultative halophyte *Mesembryanthemum crystallinum.* EMBO J **11:** 2077–2085

Yamada A, Saitoh T, Mimura T, Ozeki Y (2002) Expression of mangrove allene oxide cyclase enhances salt tolerance in *Escherichia coli*, yeast, and tobacco cells. Plant Cell Physiol **43:** 903–910